BOSTON UNIVERSITY

NIH NATIONAL CANCER INSTITUTE Early Detection Research Network

UCLA

The BU-UCLA Lung Cancer Biomarker Development Laboratory

Lung Collaborative Group

June 30th 2020

Marc Lenburg, PhD; Steven Dubinett, MD;
Denise Aberle, MD;
David Elashoff, PhD

Study Overview

Goal: **Develop predictive models that integrate clinical, molecular and imaging-based data** for lung cancer detection in older smokers **with nodules 6-25 mm** who are at elevated risk for lung cancer as a result of meeting eligibility criteria for screening.

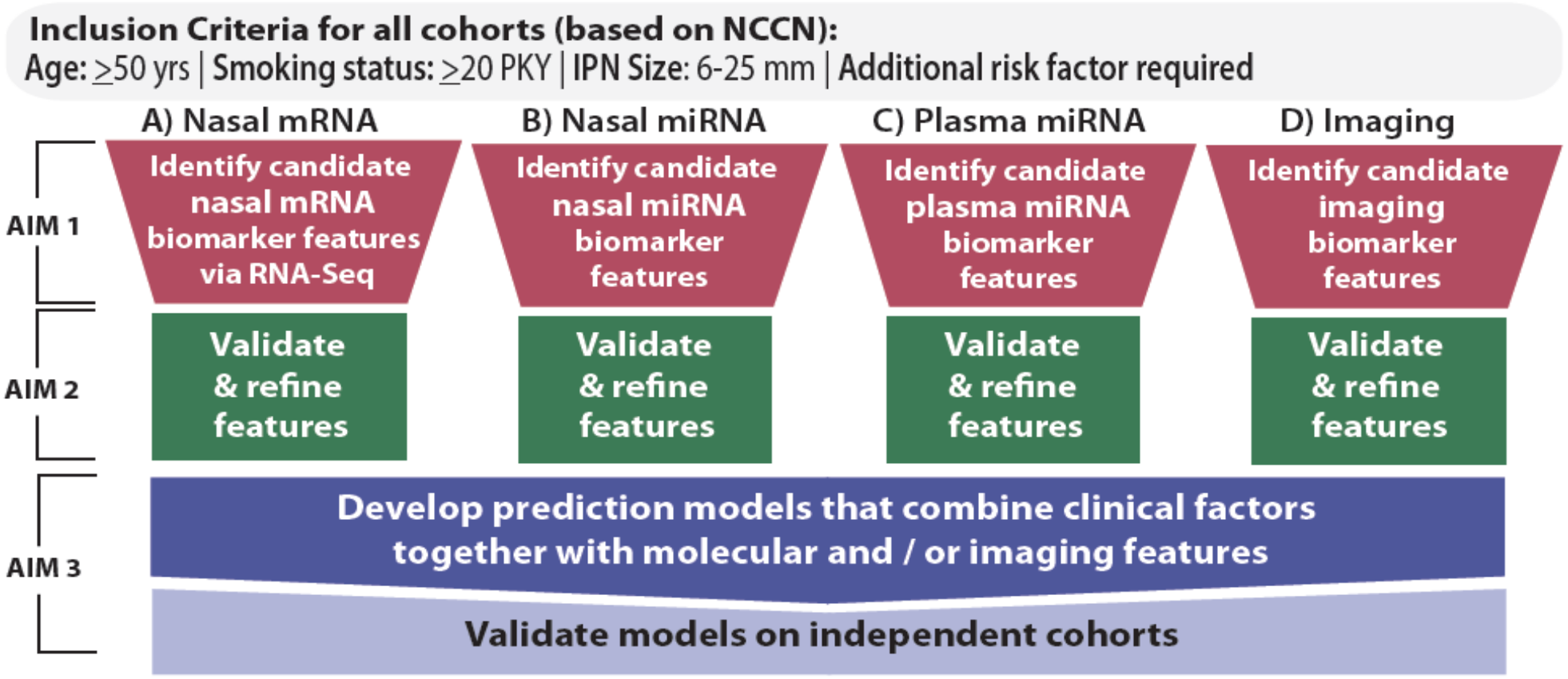

Cohorts for Aim 1

Cohorts	Aim	Number of Samples		Biospecimens		
All subjects are screen eligible (NCCN Criteria)*		Total (Cancer)	Aim Totals	Nasal	Plasma	Imaging
DECAMP I	1	200 (100)	200 (100)	✖	✖	✖

DECAMP 1 (Detection of Early Lung Cancer Among Military Personnel):

- Smokers undergoing diagnostic workup for indeterminate pulmonary nodule
- Inclusion Criteria: >45yrs of age with a minimum 20 pack-year smoking history, CT-detected solid or part-solid IPN ranging from 7-30 mm.
- Enrollment occurring from 4 military hospitals and 7 VA hospitals across the United States.

AIM 2

Aim 2: Validate and refine the molecular and imaging features identified in Aim 1 by selecting those that best discriminate malignant vs. benign indeterminate pulmonary nodules in independent cohorts.

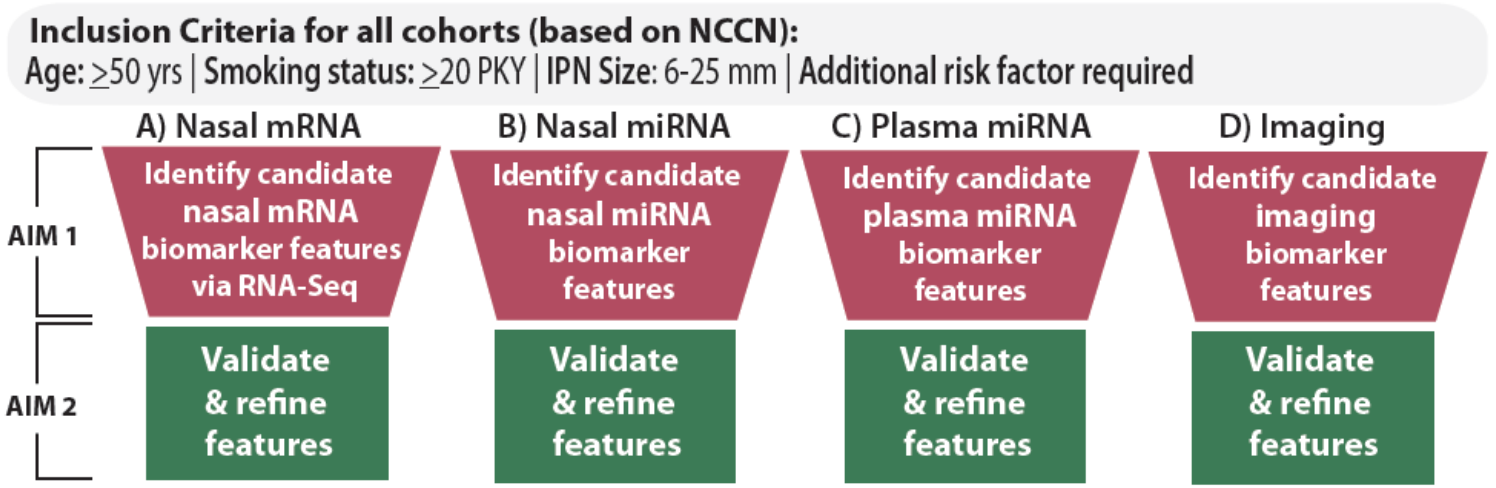

Cohorts for Aim 2

Cohorts	Aim	Number of Samples		Biospecimens		
All subjects are screen eligible (NCCN Criteria)*		Total (Cancer)	Aim Totals	Nasal	Plasma	Imaging
DECAMP I	2	100 (50)	150 (75)	✖	✖	✖
EDRN Lung Team		50 (25)		✖	✖	✖

DECAMP 1 (Detection of Early Lung Cancer Among Military Personnel):

- Smokers undergoing diagnostic workup for indeterminate pulmonary nodule
- Inclusion Criteria: >45yrs of age with a minimum 20 pack-year smoking history, CT-detected solid or part-solid IPN ranging from 7-30 mm,
- Enrollment occurring from 4 military hospitals and 7 VA hospitals across the United States.

EDRN Lung Team:

- Smokers undergoing diagnostic workup for indeterminate pulmonary nodule
- Inclusion Criteria: >45yrs of age with a minimum 20 pack-year smoking history, CT-detected solid or part-solid IPN ranging from 7-25 mm.
- Enrollment occurring from 4 academic institutions: BU, UCLA, Vanderbilt, NYU

AIM 3

Aim 3: Develop and validate prediction models for indeterminate pulmonary nodule malignancy that combine clinical factors together with molecular and/ or imaging features.

A. Develop prediction models that integrate molecular and/or imaging features from Aim 2 in combination with clinical factors using multiple prospective cohorts of screen-detected and screen-eligible incidental indeterminate pulmonary nodules**.**
B. Validate the integrated models in independent patients from these cohorts.

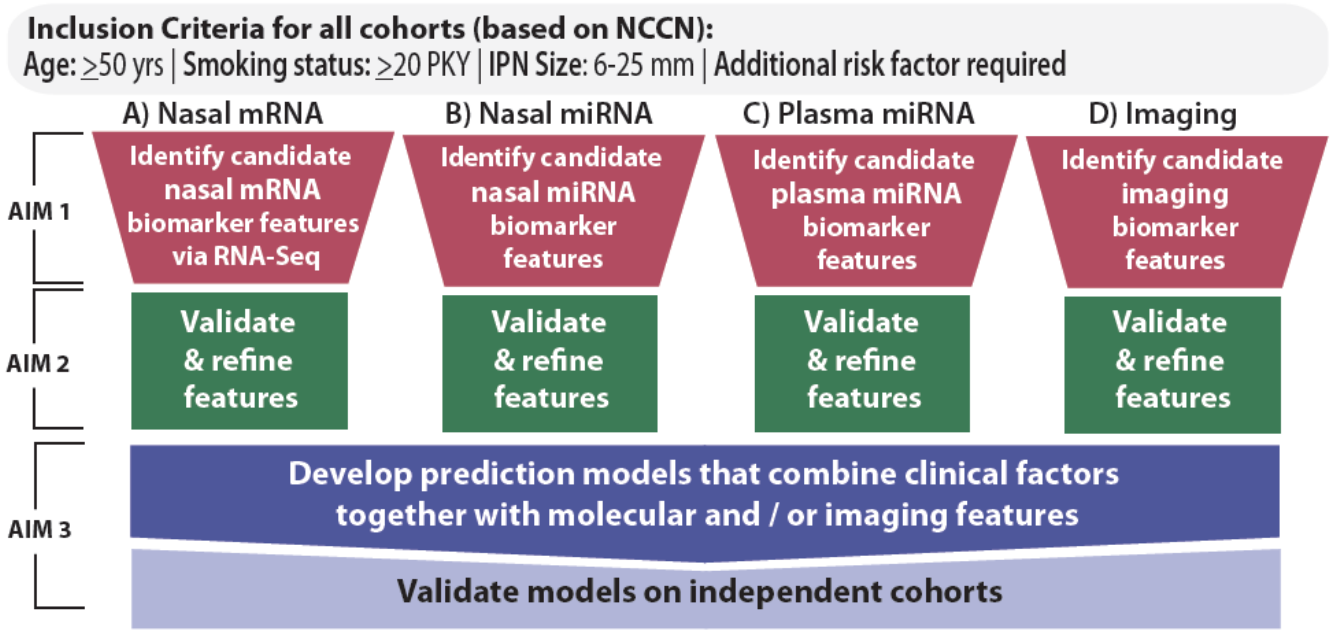

Aim 1A: Nasal epithelial gene expression signature associated with lung cancer diagnosis in the indeterminate nodule setting

128 DEGs, FDR q<0.05

58 Benign 104 Cancer

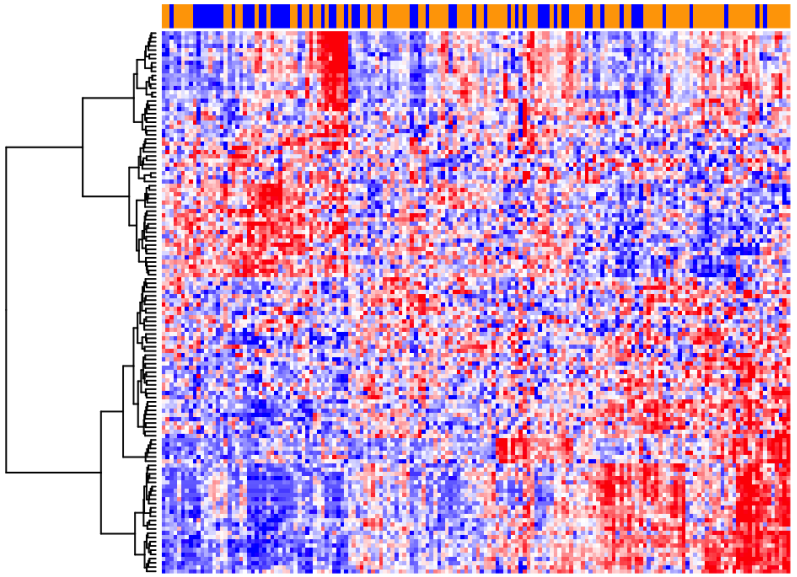

DECAMP 1 Cohort N=162
(Discovery)

Replication

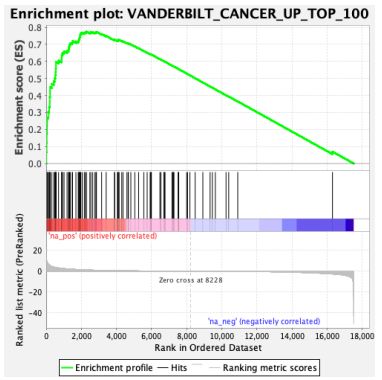

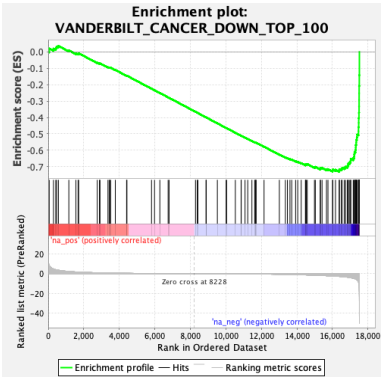

Vanderbilt
N=59

J. Zhang, BU
P. Massion, Vanderbilt

Distribution of cancer-biomarker genes among nasal epithelial cells

Genes increased in lung cancer patients

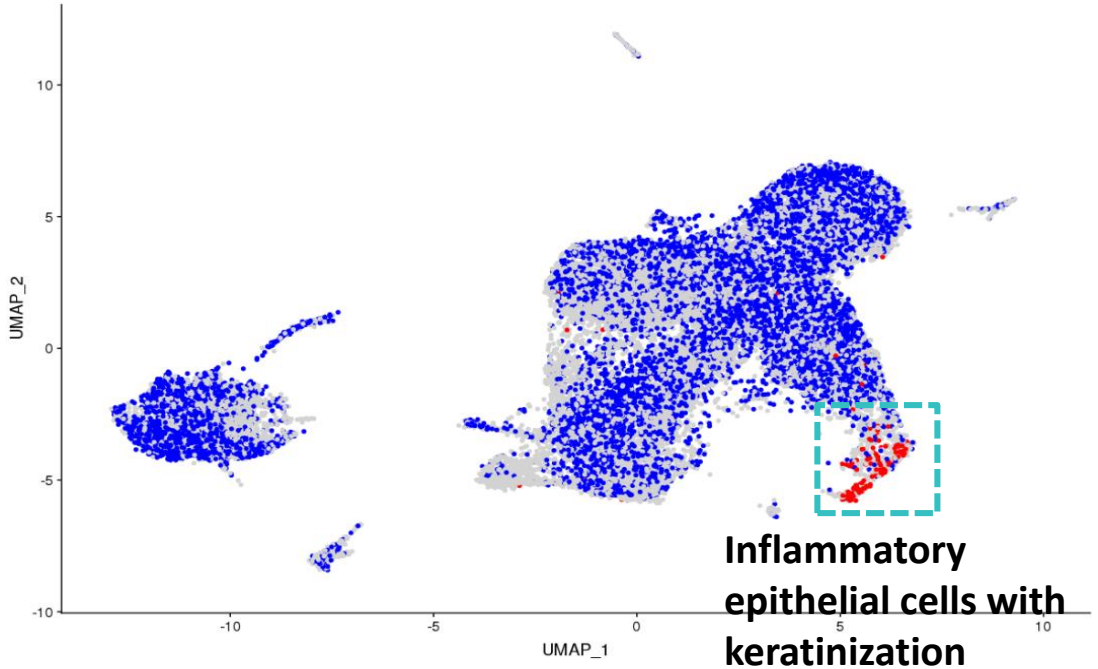

Genes decreased in lung cancer patients

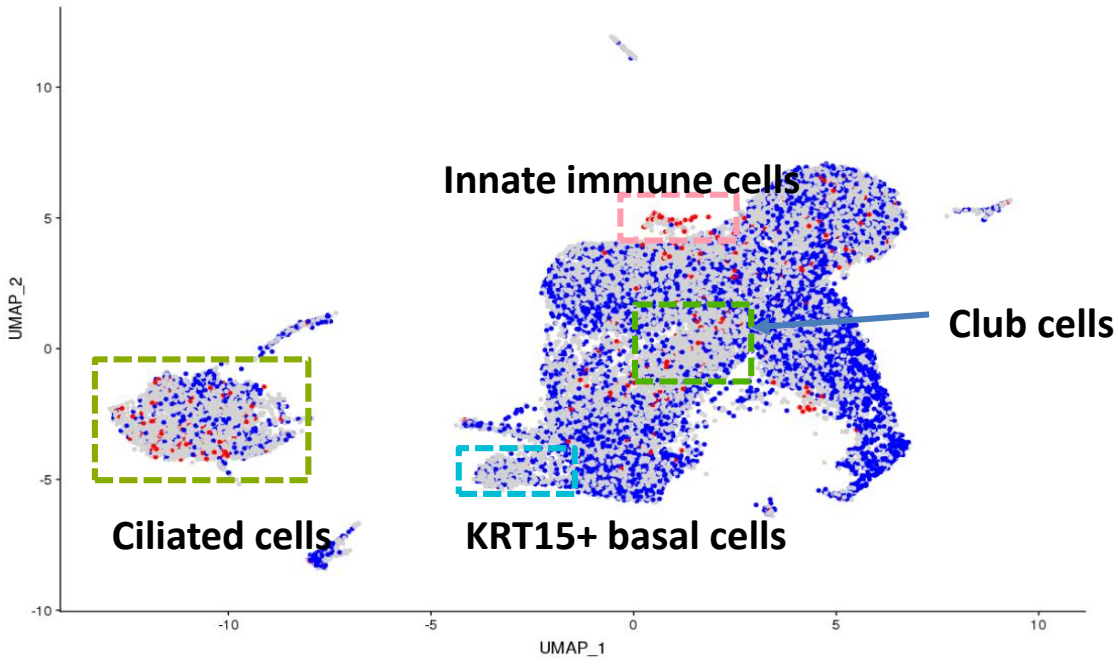

N = 6 subjects with IPN, ~40,000 cells

K. Christ, C. Lamb, Lahey
Xu Ke, BU

Funded via SU2C

Aim 1B: miRNA with lung cancer associated expression in nasal epithelium

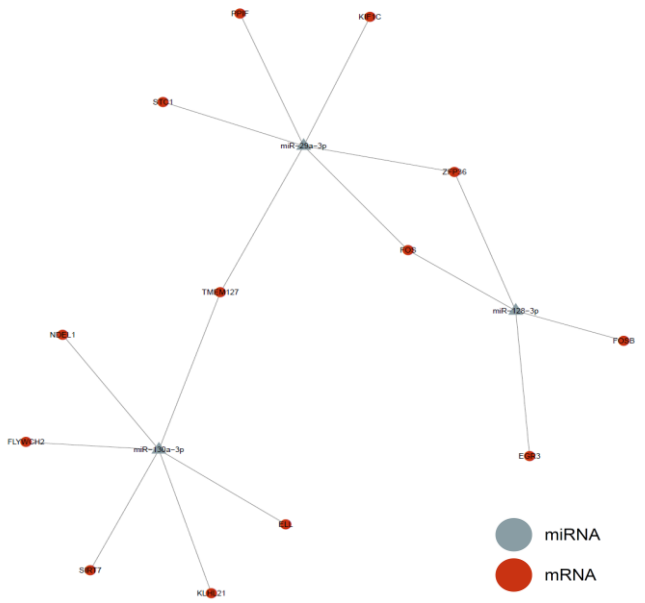

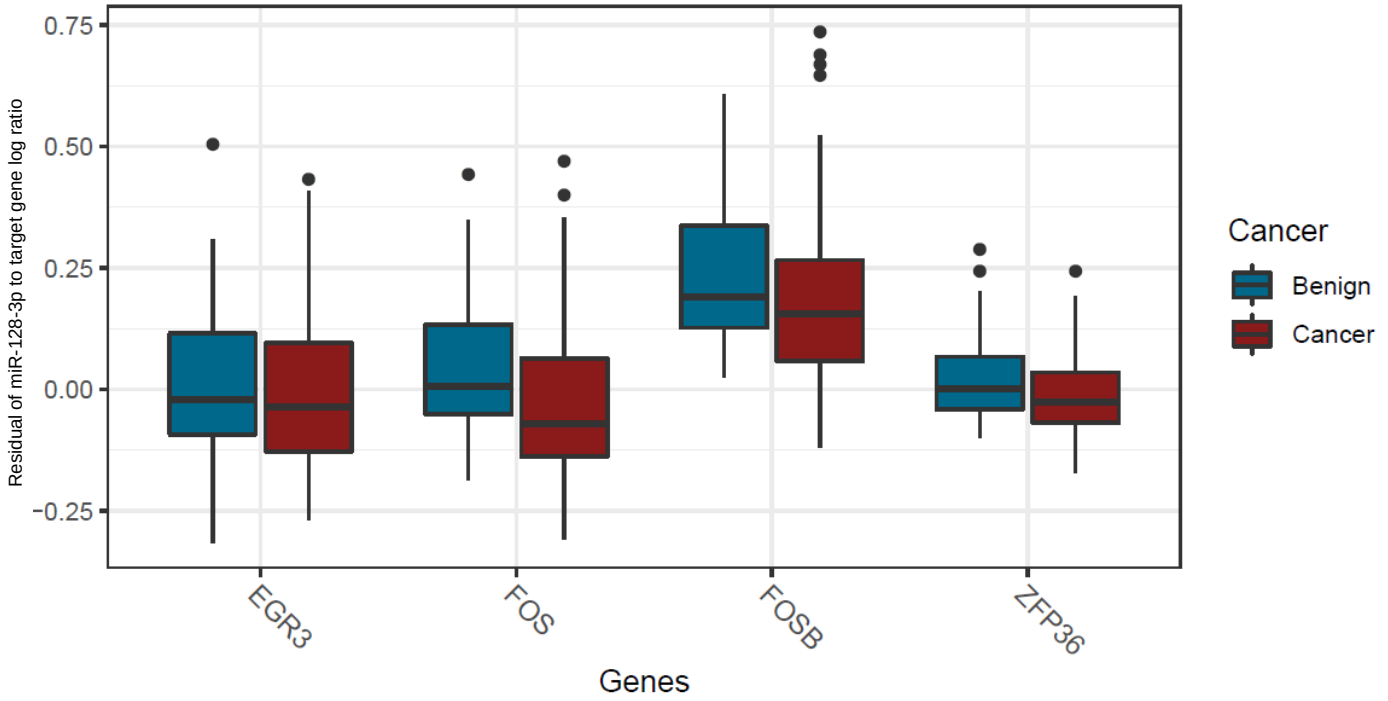

- miRNAseq of 179 DECAMP1 nasal samples
- Identification of miRNA negatively correlated with predicted mRNA targets (FDR < 0.05)
- Identify three miRNA whose targets are enriched for mRNA with cancer-associated expression
- One of these (miR-128-3p) replicates in independent cohort from Lahey (n=64)

Boting Ning, BU

Aim 1C: Plasma miRNA

MiRXES platform utilized for estimating plasma miRNAs

Detected range: 10^2 to 10^8 copies/ml serum

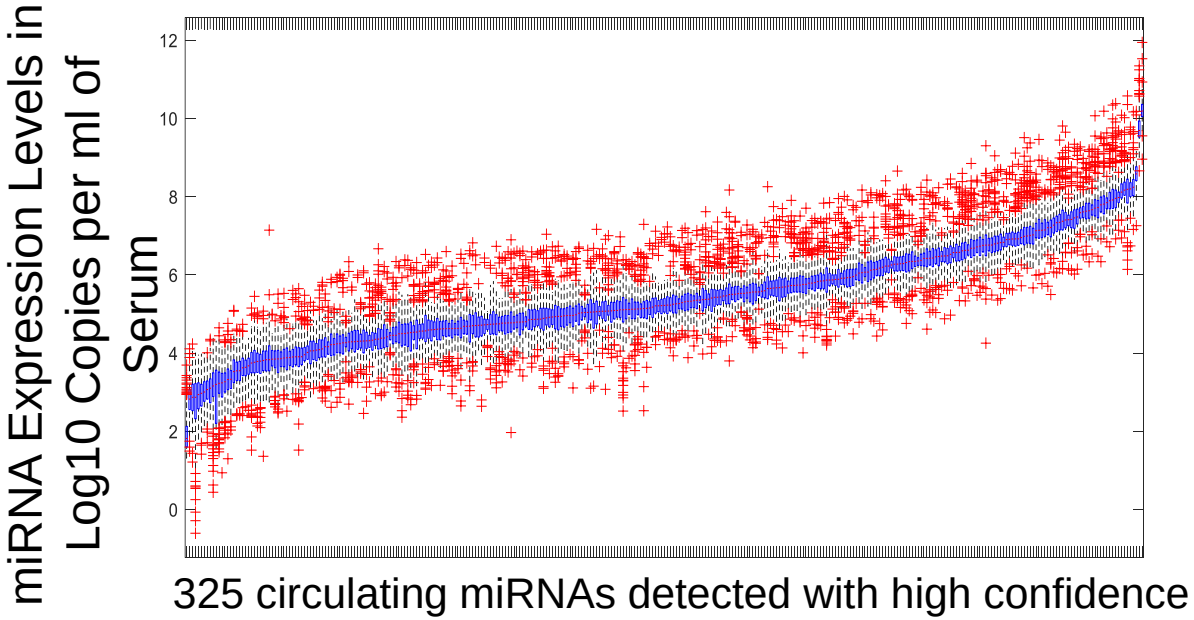

325 circulating miRNAs detected with high confidence

Hemolysis impacts miRNA profile

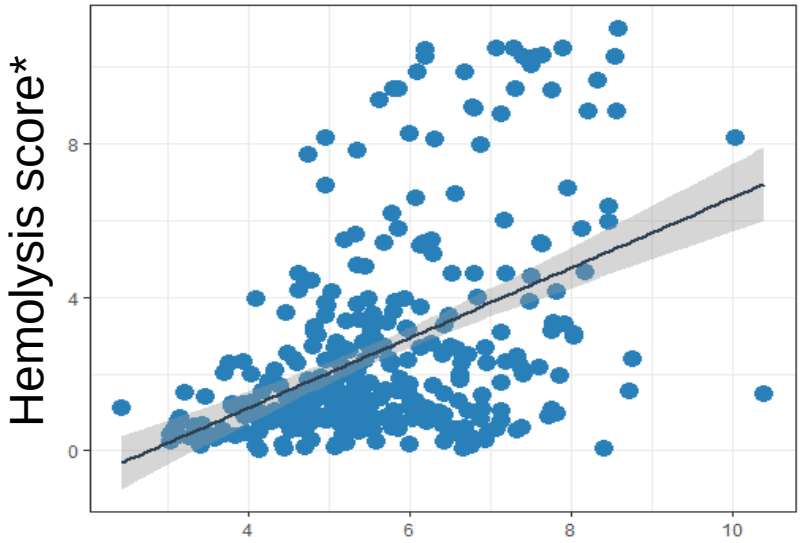

- MiRXEs platform utilizes RT-qPCR technology with spike-in RNAs to control variation in each step from miRNA isolation to replication.
- The platform detects miRNA at a dynamic range of 10^2 to 10^8 copies/ml serum.
- The platform detected 325 target miRNAs in this cohort.
- miRNA in plasma is sensitive to hemolysis and thus requires extra care in sample procurement.

***Hemolysis score** is the log-transform of FDR of Kruskal-Wallis test justifying the association between miRNA and hemolysis levels

Study cohort demographic and clinical features

Feature	Benign	Cancer	p-value
Number*	90	91	
Mean age	67.2	68.2	0.65
Females – no. (%)	22 (24.4%)	16 (17.6%)	0.43
Mean nodule size (cm)	1.27	1.46	0.0014
Smoking Status – no. (%)			
Current	33 (36.7%)	39 (42.9%)	0.13
Former	49 (54.4%)	50 (54.9%)	
Unknown	8 (8.9)	2 (2.2%)	
Race – no. (%)			
Caucasian	65 (72.2%)	70 (76.9%)	0.012
African American	10 (11.1%)	18 (19.8%)	
Asian	3 (3.3%)	0 (0.0%)	
Other	12 (12.3%)	3 (3.2%)	

Distribution of nodule size

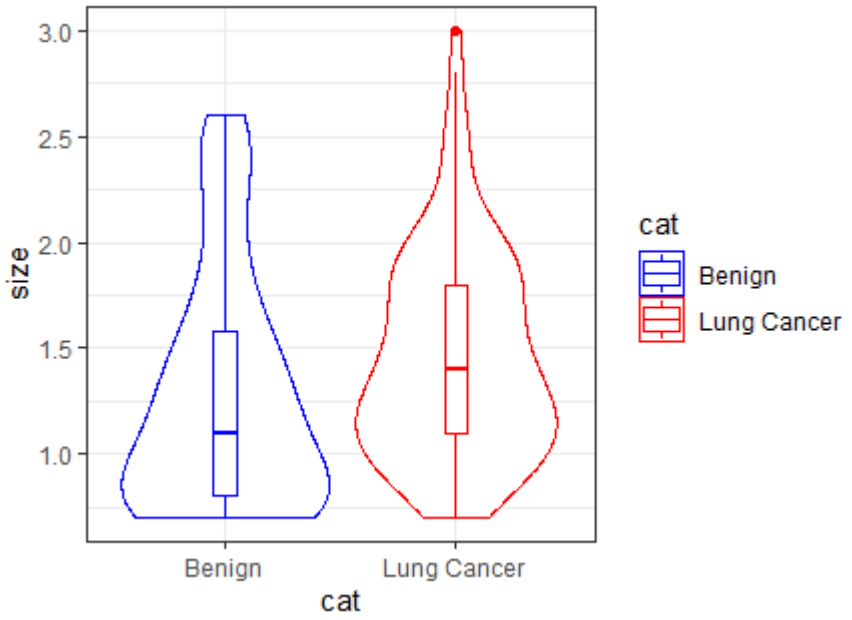

*After removing hemolyzed samples

Differentially expressed miRNAs

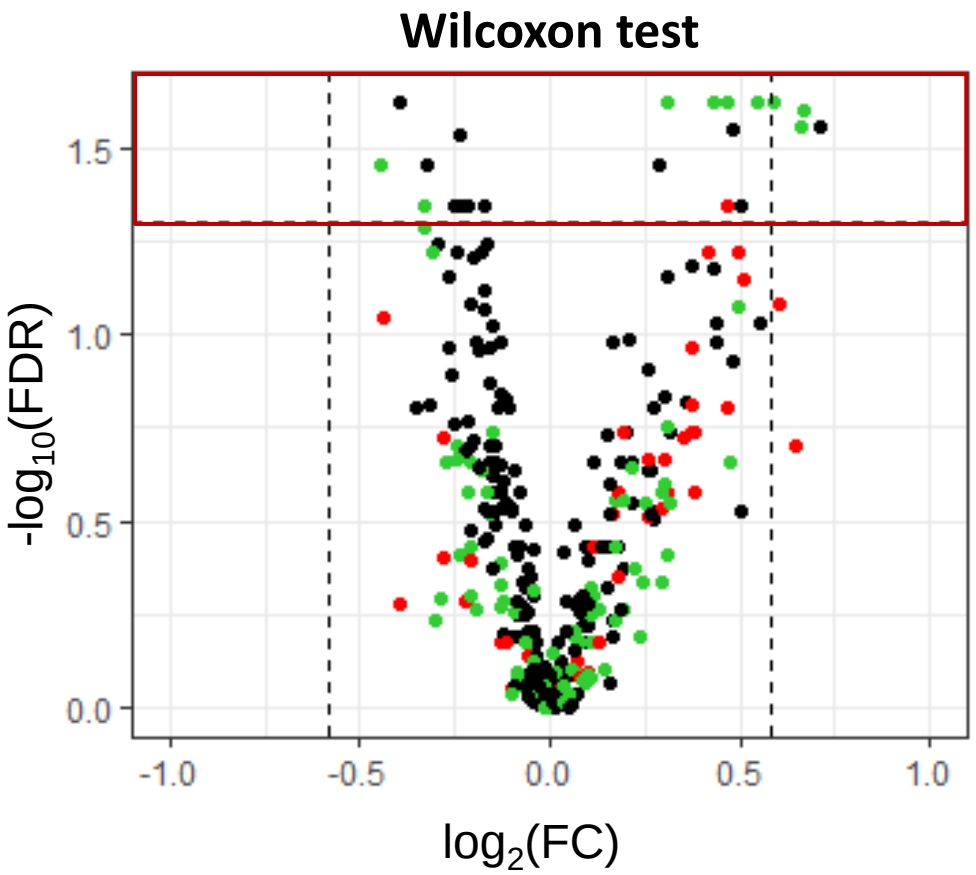

- <1% missing data points
- 1%-10% missing data points
- > 10% missing data points

miRs	Log_2(FC)	PV	FDR	Abundance in Normal Plasma/Blood Cells*
hsa-let-7f-5p	-0.40	3.17E-04	0.024	high
hsa-miR-1207-5p	0.50	2.73E-03	0.045	
hsa-miR-141-3p	0.47	3.46E-04	0.024	
hsa-miR-151a-5p	-0.25	2.51E-03	0.045	high
hsa-miR-200a-3p	0.59	3.99E-04	0.024	
hsa-miR-205-5p	0.71	7.27E-04	0.028	
hsa-miR-339-3p	-0.44	1.48E-03	0.035	
hsa-miR-34a-3p	0.43	4.16E-04	0.024	
hsa-miR-374a-5p	-0.24	9.97E-04	0.029	
hsa-miR-375	0.66	7.65E-04	0.028	
hsa-miR-450a-5p	0.48	8.65E-04	0.028	
hsa-miR-596	0.29	1.51E-03	0.035	
hsa-miR-616-5p	0.31	2.44E-04	0.024	

*PMID: 22158052

Differentially expressed miRNAs – frequently selected as top DEGs

miRs	log2_FC	FDR	Abundance (avg copies per mL)
hsa-let-7f-5p	-0.40	0.024	5.40E+07
hsa-miR-1207-5p	0.50	0.045	2.10E+05
hsa-miR-141-3p	0.47	0.024	5.40E+05
hsa-miR-151a-5p	-0.25	0.045	6.50E+06
hsa-miR-200a-3p	0.59	0.024	1.90E+05
hsa-miR-205-5p	0.71	0.028	1.30E+05
hsa-miR-339-3p	-0.44	0.035	5.20E+04
hsa-miR-34a-3p	0.43	0.024	1.80E+04
hsa-miR-374a-5p	-0.24	0.029	9.70E+06
hsa-miR-375	0.66	0.028	1.70E+05
hsa-miR-450a-5p	0.48	0.028	7.60E+05
hsa-miR-596	0.29	0.035	3.10E+04
hsa-miR-616-5p	0.31	0.024	1.20E+05

Selected as top 10 genes

>90/100

70-90/100

- DEGs were assessed by randomly selecting subsets (90% of total samples) to determine if these identified miRNAs can utilized as biomarkers
- 5 miRNAs were frequently (>90/100 permutations) selected in the top 10 miRNAs.
- 4 miRNAs appeared frequently (70-90/100) in the top 10 rank miRNAs

→ Nine miRNAs with stable expression associated with lung cancer

Compared to plasma miRNA-Seq data sets

miRs	log2_FC	FDR	Abundance (avg copies per mL)	PV		
				UCLA miR-seq		BU miR-seq
				Tumor ≤ 2cm	Tumor > 2cm	
hsa-let-7f-5p	-0.40	0.024	5.40E+07	0.71	0.57	0.25
hsa-miR-1207-5p	0.50	0.045	2.10E+05	N/A	N/A	N/A
hsa-miR-141-3p	0.47	0.024	5.40E+05	0.41	**0.03**	**0.01**
hsa-miR-151a-5p	-0.25	0.045	6.50E+06	0.30	0.64	0.10
hsa-miR-200a-3p	0.59	0.024	1.90E+05	0.27	**0.07**	**0.01**
hsa-miR-205-5p	0.71	0.028	1.30E+05	0.01	0.004	0.61
hsa-miR-339-3p	-0.44	0.035	5.20E+04	0.78	0.24	0.87
hsa-miR-34a-3p	0.43	0.024	1.80E+04	N/A	N/A	N/A
hsa-miR-374a-5p	-0.24	0.029	9.70E+06	0.39	0.01	0.19
hsa-miR-375	0.66	0.028	1.70E+05	0.60	**0.05**	**0.03**
hsa-miR-450a-5p	0.48	0.028	7.60E+05	0.40	0.03	0.64
hsa-miR-596	0.29	0.035	3.10E+04	N/A	N/A	N/A
hsa-miR-616-5p	0.31	0.024	1.20E+05	0.45	0.11	N/A

- Plasma miRNA-Seq was performed on *two different cohorts* of patients with benign and malignant pulmonary nodules
- Most of nine miRNAs identified in the current study were also differentially expressed in miRNA-Seq data in tumors > 2cm

Selected as top 10 genes

>90/100

70-90/100

Potential biological roles of detected miRNAs

miRs	log2_FC	FDR	PV			Literature
			UCLA miR-seq		BU miR-seq	
			Tumor ≤ 2cm	Tumor > 2cm		
hsa-let-7f-5p	-0.40	0.024	0.71	0.57	0.25	down in NSCLC (PMID: 20595154)
hsa-miR-1207-5p	0.50	0.045	N/A	N/A	N/A	
hsa-miR-141-3p	0.47	0.024	0.41	**0.03**	**0.01**	Poor prognosis in early state ADC (PMID: 25003366)
hsa-miR-151a-5p	-0.25	0.045	0.30	0.64	0.10	
hsa-miR-200a-3p	0.59	0.024	0.27	**0.07**	**0.01**	Regulating EMT,
hsa-miR-205-5p	0.71	0.028	0.01	0.004	0.61	Regulating EMT, ADC specific miRNA (PMID: 25695220)
hsa-miR-339-3p	-0.44	0.035	0.78	0.24	0.87	
hsa-miR-34a-3p	0.43	0.024	N/A	N/A	N/A	
hsa-miR-374a-5p	-0.24	0.029	0.39	0.01	0.19	Targeting PTEN in late stage NSCLC (PMID:29362431)
hsa-miR-375	0.66	0.028	0.60	**0.05**	**0.03**	SCC specific miRNA (PMID: 25695220)
hsa-miR-450a-5p	0.48	0.028	0.40	0.03	0.64	
hsa-miR-596	0.29	0.035	N/A	N/A	N/A	
hsa-miR-616-5p	0.31	0.024	0.45	0.11	N/A	

Selected as top 10 genes

>90/100

70-90/100

Summary

- We identified nine plasma miRNAs detected as significantly different between benign and cancer nodules by utilizing the MiRXES platform
- These miRNAs were also differentially expressed in two independent sequencing data sets
- Their expression was associated with nodule size, which should be incorporated in building classifiers
- Future studies can address the importance of detected miRNAs in impacting lung cancer development and progression

Image Analysis & Radiogenomics in NSCLC

Semantic Analysis

Engineered radiomic features

Deep learning & Radiogenomics

Denise R. Aberle, MD
Professor of Radiology and Bioengineering
Vice Chair for Research | Radiological Sciences
David Geffen School of Medicine at UCLA

Semantic analysis

- Textual descriptions based on visualization
  - Nodule: Consistency | location | margins | shape | internal features *and* nodule surround
  - Addressing moderate reader variability
- Semantic Reader study | 90 test cases of indeterminate lung nodules
  - Description of Illustrated lexicon & Training Manual
  - Launching multi-reader study pre- & post-training to improve reader agreement
  - Images are fully annotated | De-identified | Pathologic truth

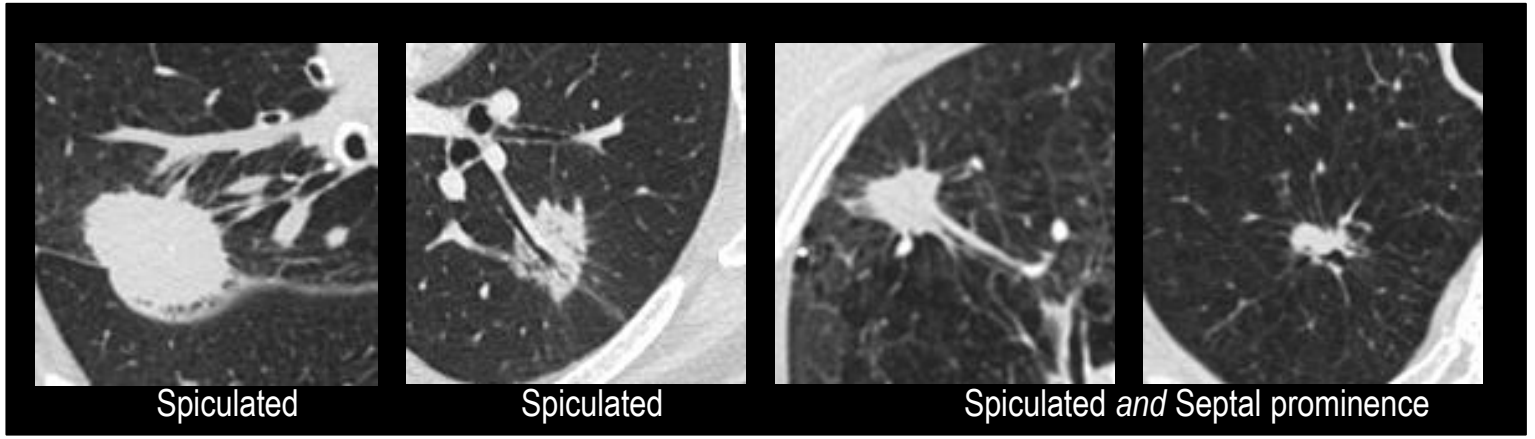

Radiomics | Engineered features

- Quantitative mathematical features
  - Types: Morphologic | Pixel intensity histogram statistics | Textures (GLCM, GLRL) Wavelet transformations derived from 3D segmentation
  - Two feature categories: Nodule | Peri-nodule surround (≤15 mm from border)
  - Susceptibility to imaging parameters
- Radiomics Progress (Cancer vs. no Cancer)
  - DECAMP 1: N = 350 cases with semantic & radiomic feature extraction
  - Data is in statistical analysis at Brown University (DECAMP) | Regression modeling

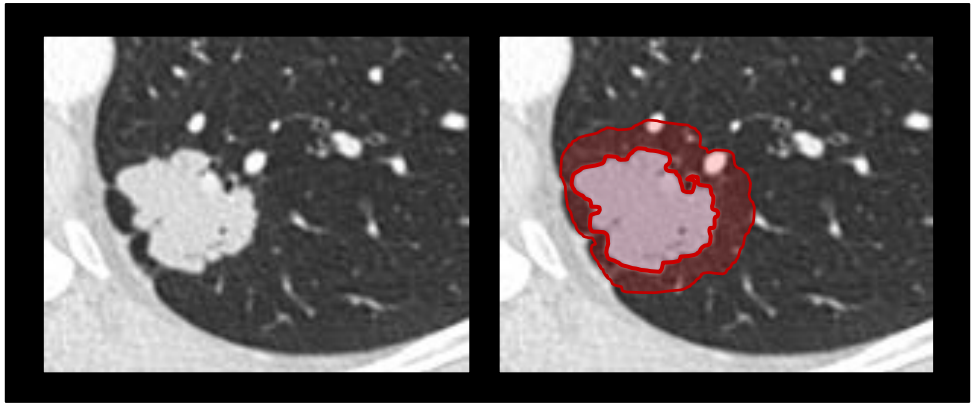

Interpretable Deep Learning

- Trained 3D CNN for nodule classification using LIDC dataset of benign & malignant nodules
- Trained hierarchical CNN to also predict semantic labels
- Compared the CNN to hierarchical semantic network:
  - 3D single CNN AUC = 0.847 (± 0.024)
  - 3D hierarchical semantic network
    AUC = 0.856 (± 0.026)
  - Mean difference between models = 0.005
    (95% CI: 0.0051-0.0129); p = 0.009

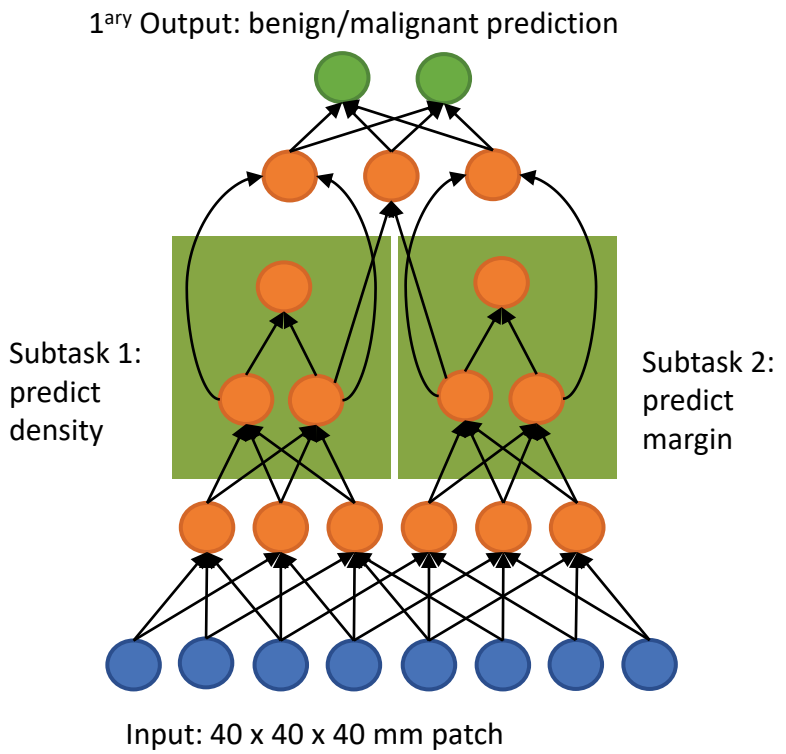

Shen S et al. Expert Syst Appl. 2019; 128:84-95.

Radiogenomics in NSCLC

- To investigate the use of deep feedforward CNN to learn associations between tumor gene expression & radiomic features | histology | stage in NSCLC
- Training (N = 262) North American | Testing (N = 89) Netherlands
- Training dataset
  - Affymetrix microarray chip | 21,766 gene expressions
  - CNN trained using 1 transcriptome for each of 7 *types* of radiomic features individually
  - Best performing hyper-parameters for any type were applied to predict a *single* radiomic feature.
  - Radiomic features with AUC ≥ 0.70 were kept
  - CNNs compared with LR, SVM, RF, gradient boosted trees

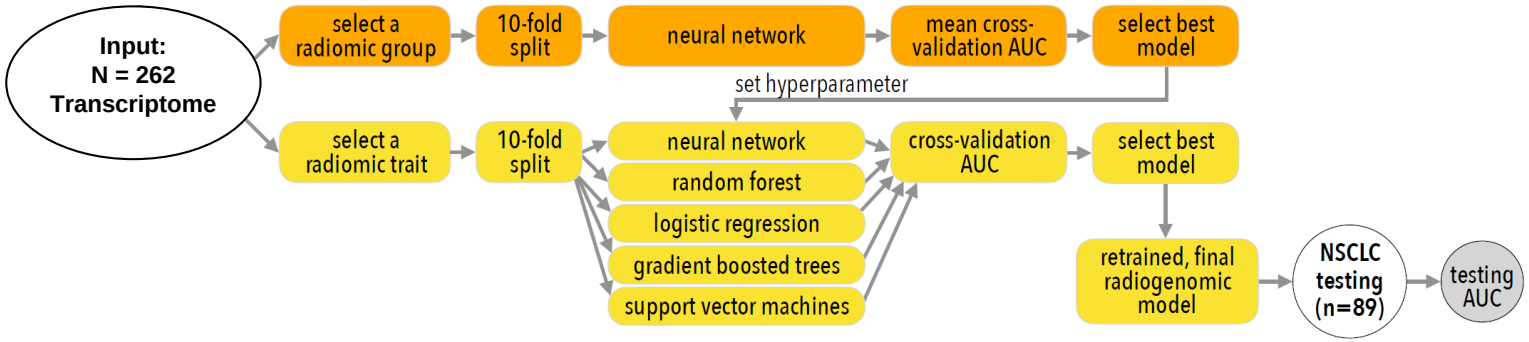

Grossman P et al. eLife 2017; 6:e23421.

Extracting predictive gene expression patterns

- Gene masking to predict radiomic features based on input of one gene set

  Predefined Hallmark & Gene Ontology biological processes gene sets from MSigDB

- Radiogenomic associations were based on highest performance (AUC)
- Also predicted histology relationships using gene masking

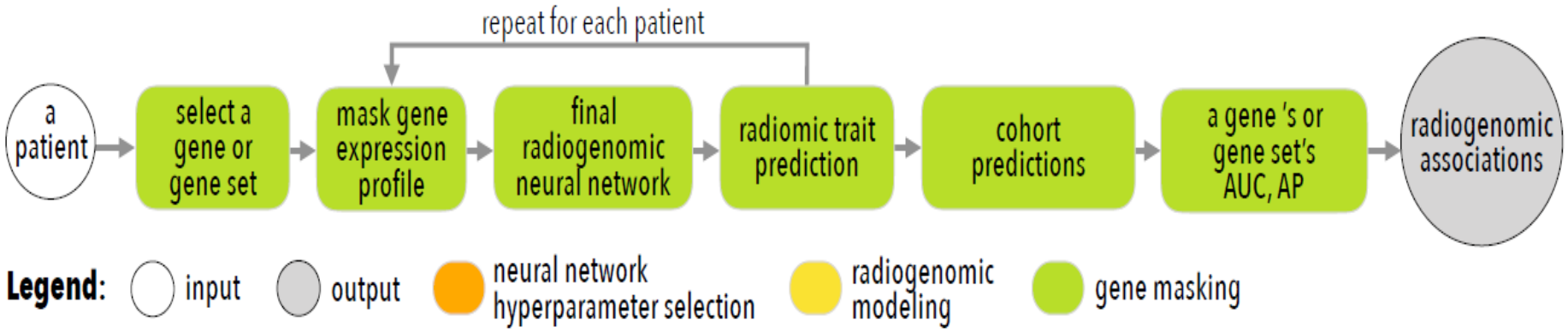

Gene expression is predictive of histology

- CNN had lowest mean error in training
  - In testing, overall AUC for histology prediction was 0.77 when microaveraged
  - ADC: AUC = 0.86
  - SCC: AUC = 0.91
  - Other histology: AUC = 0.71

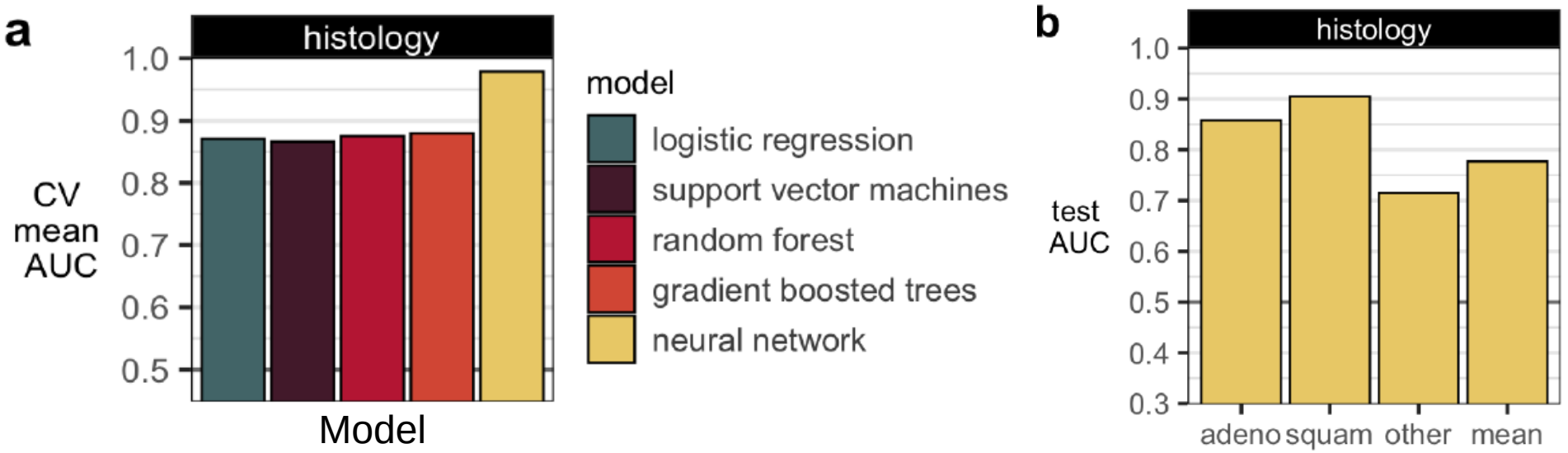

Gene masking identifies Hallmark gene sets predictive of histology

- Hypoxia | coagulation | *KRAS* signaling could predict both ADC and SCC AUC > 0.90

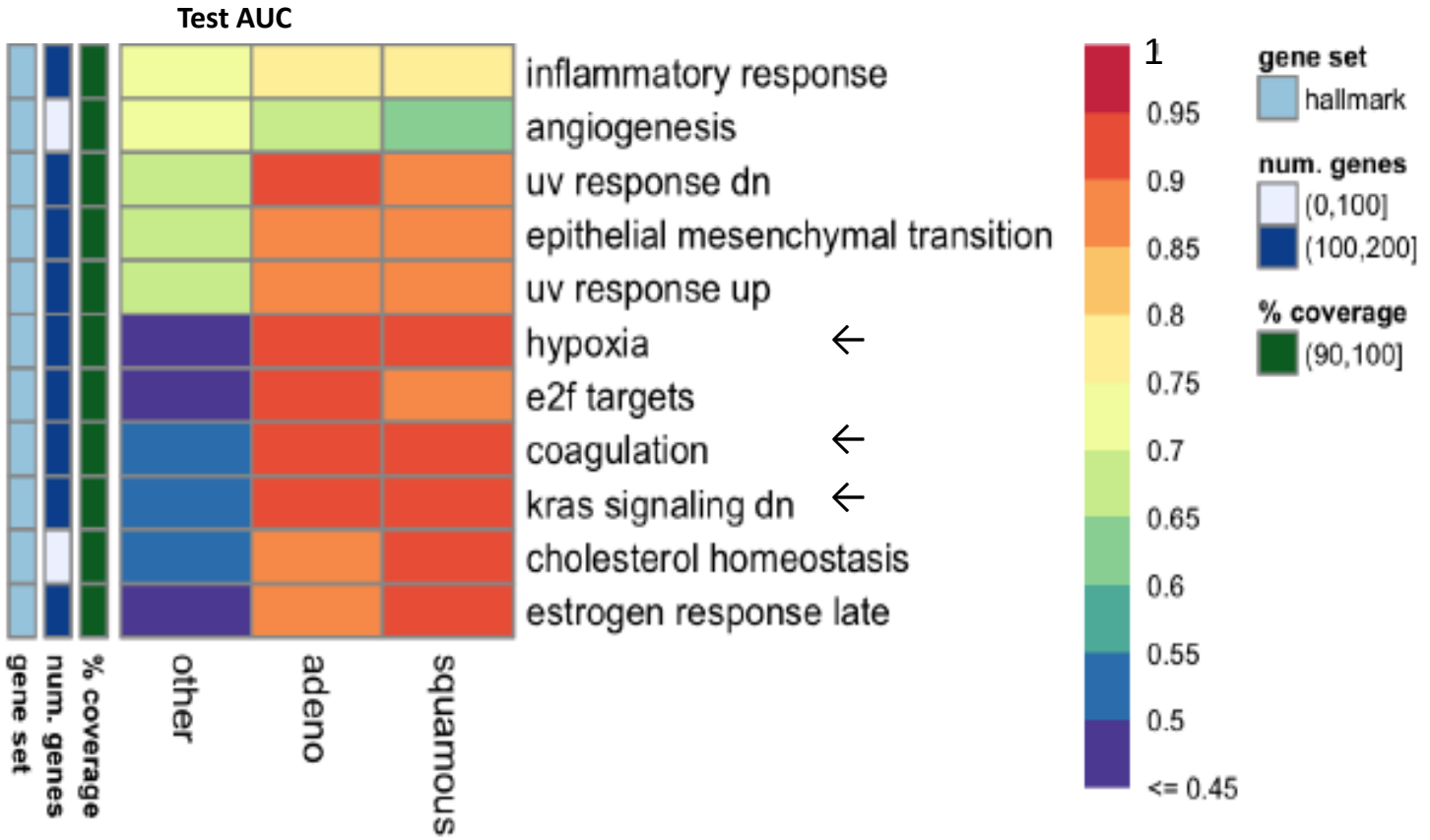

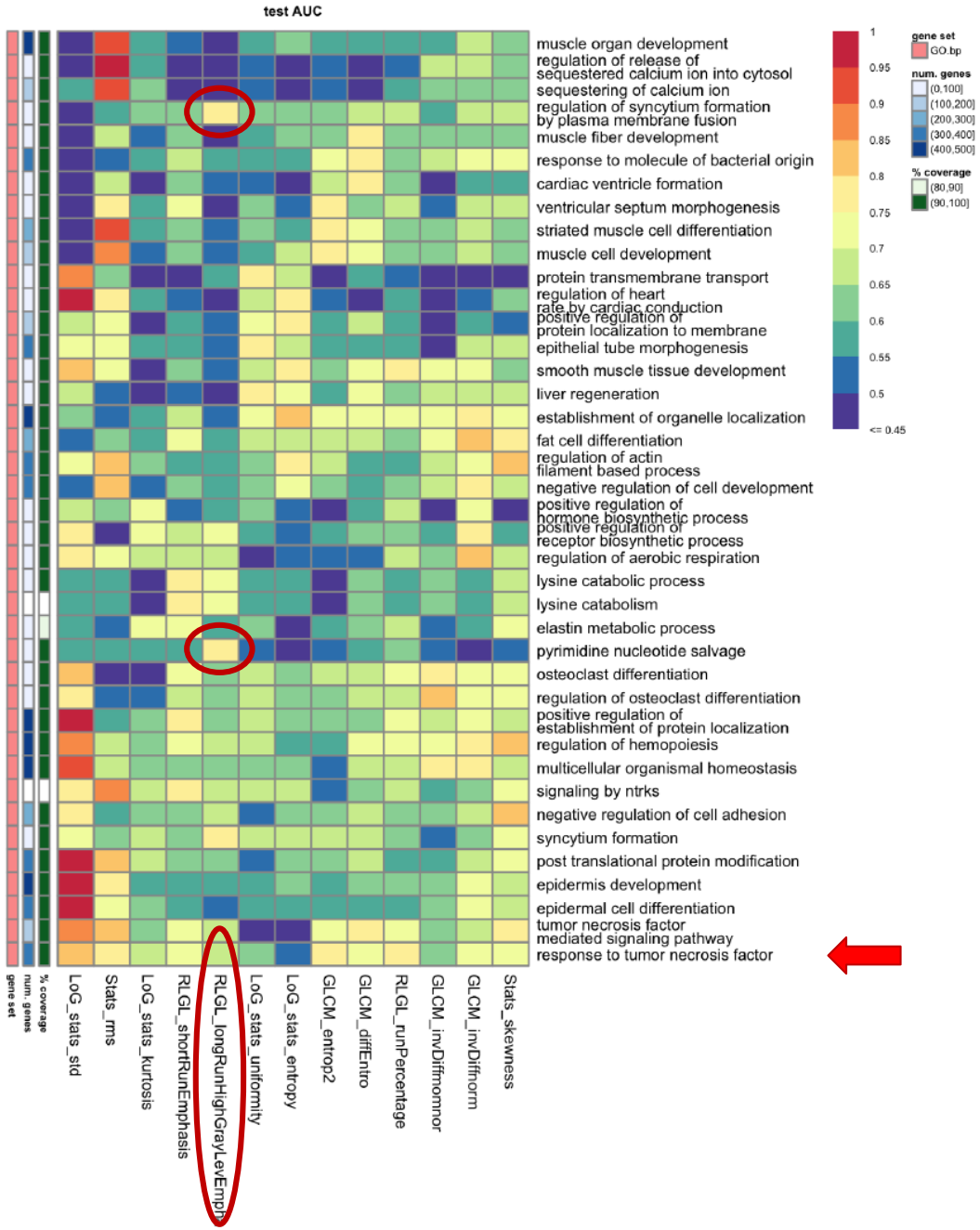

Predicting radiomic features from gene sets

- CNN out performed other models
- 13 radiomic features had testing AUC ≥ 0.70
  - Gene sets may be exclusive to one radiomic feature
  - Some gene sets predict multiple radiomic features
- Radiogenomic modules (correlated radiomic-gene expressions) were also found in Grossman et al, but there are differences between these two studies

Grossman P et al. eLife 2017; 6:e23421.

Datasets for diagnostic and prognostic prediction with DL

- NLST (N > 1500 images, enriched for lung cancer | Nodule 6-25 mm
  - Segmentation for radiomic feature extraction
  - Semantic analysis (2 readers)
- DECAMP 1 dataset (N ~450)
- Percutaneous biopsy patients (biospecimen collection) N = 300 LCs
  - Screening cohort
  - Ever smokers
  - Never smokers

EDRN Set asides: Nasal/Blood Biomarkers Pre/Post Surgery

Clinical Leads Kei Suzuki (BU) and Jane Yanagawa (UCLA)

Goal: Examine the **reversibility of lung cancer associated** nasal gene expression and blood-based **biomarkers following lung cancer resection**.

Study Design

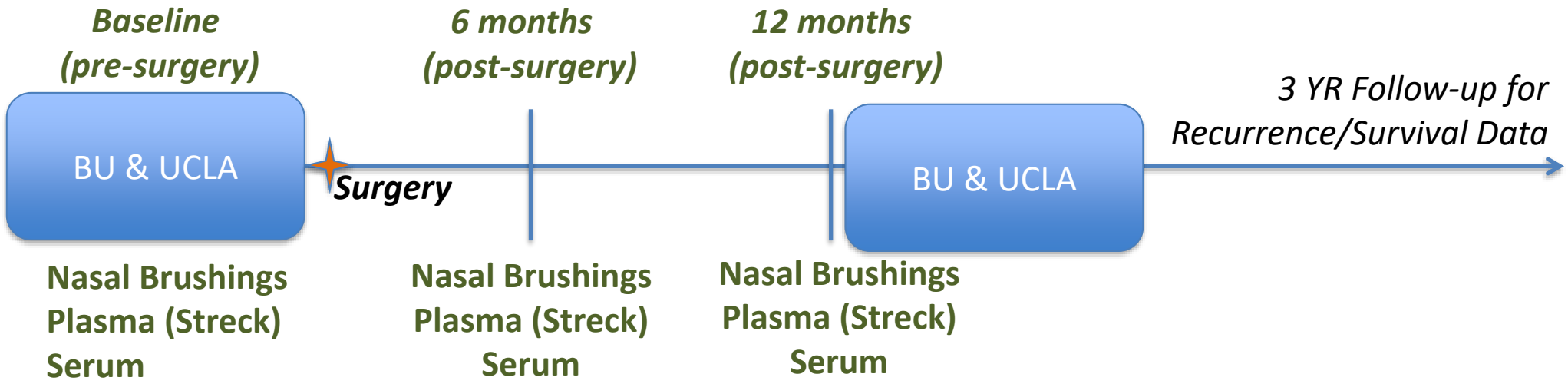

Enrollment Progress to-date

- BU: 12
- UCLA: 24

Additional Studies:

- Tumor WES
- MIF
- cfDNA
- Single cell transcriptome

Leverages new VA funding for cohort expansion in collaboration with Vanderbilt and Colorado

Future Plans

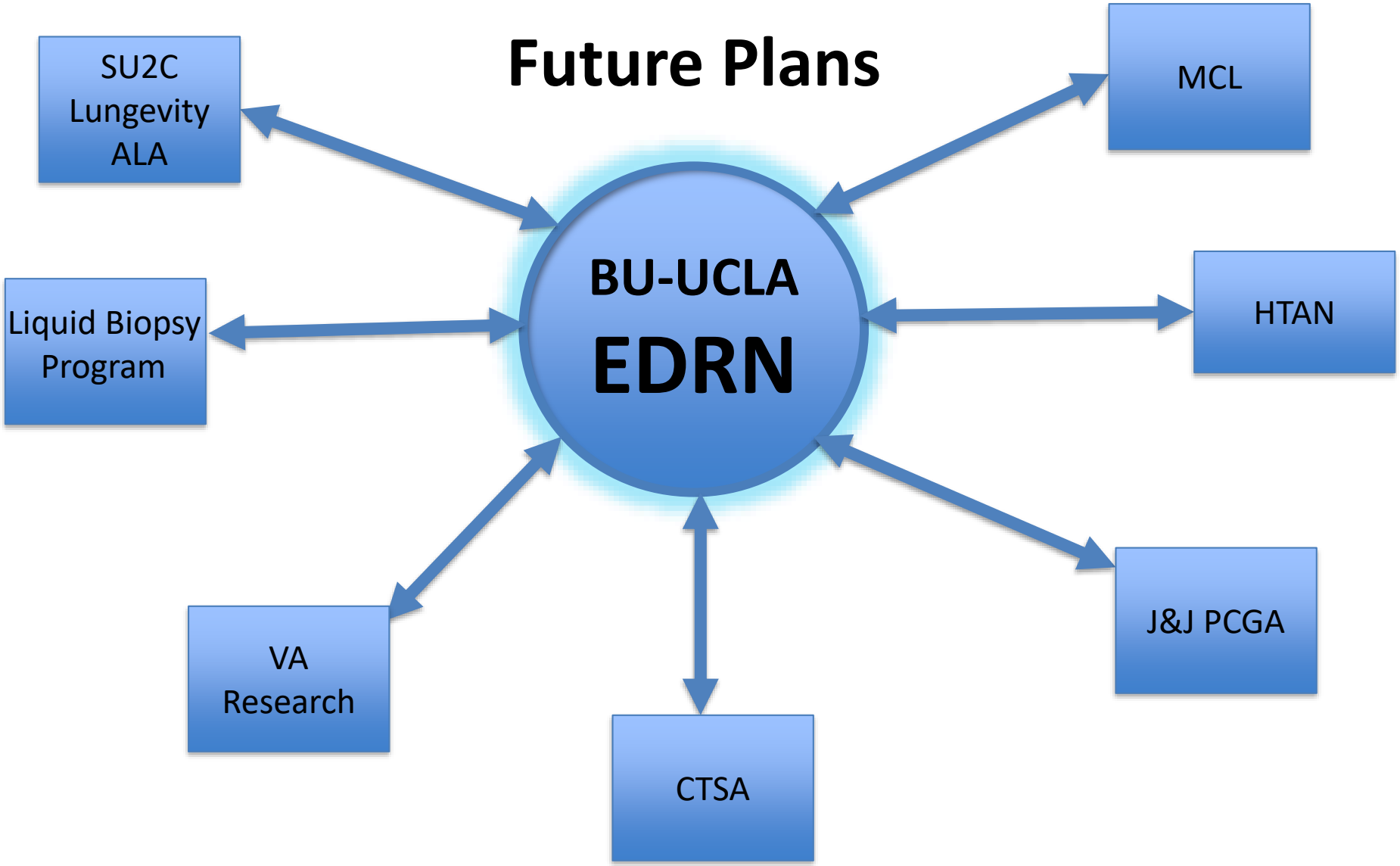

Focus on:

- **high risk populations**
- **understanding the pathogenesis of lung cancer to facilitate early detection and interception**

Early detection of recurrence from post-surgery cancer patients

Limitation on current methods

- Tracking a small number of mutations — **whole-exome sequencing**
- Unable to detect 2nd primary — **novel mutation identification**
- **Low-level tumor signal** — **machine learning**

A recent study used WGS for recurrence monitoring

Genome-wide cell-free DNA mutational integration enables ultra-sensitive cancer monitoring

Ziran et al. Nature Medicine, June 1, 2020

Our approach: increasing signal-to-noise ratio by removing sequencing errors

Identify clonal mutations at baseline

↓

Classify read pairs containing true variants and sequencing errors

↓

Build background noise distribution using random genomic locations

↓

Predict recurrence by comparing variant read counts with background

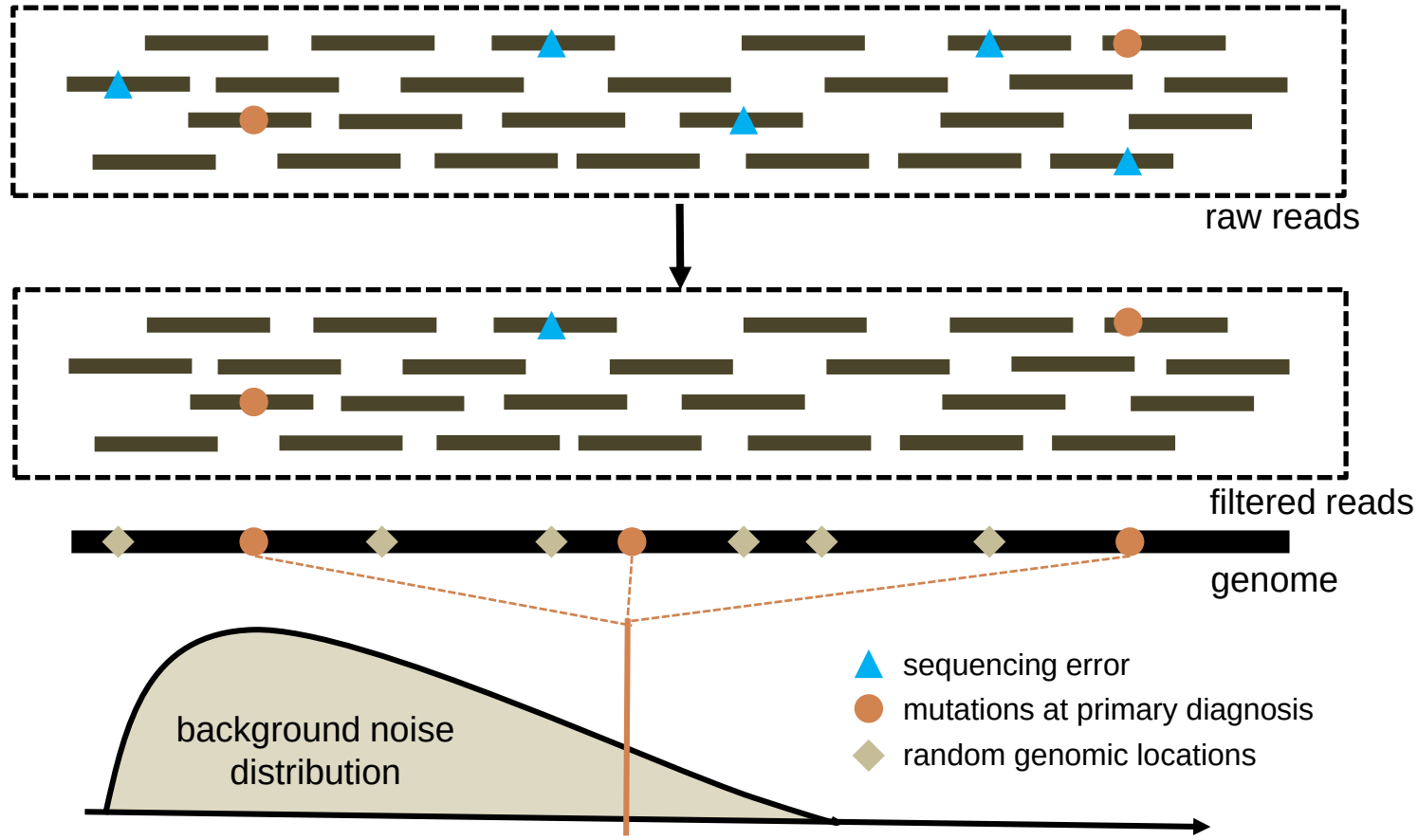

Simulation results: Sensitive detection of recurrence at tumor fraction 0.025%

- 919 simulation cases with tumor fraction 0% to 0.25%
  - 50 remission + 869 recurrence
- The performance improves as the sequencing depth is higher
- AUC > 90% when tumor fraction >= 0.025% at 200x sequencing depth

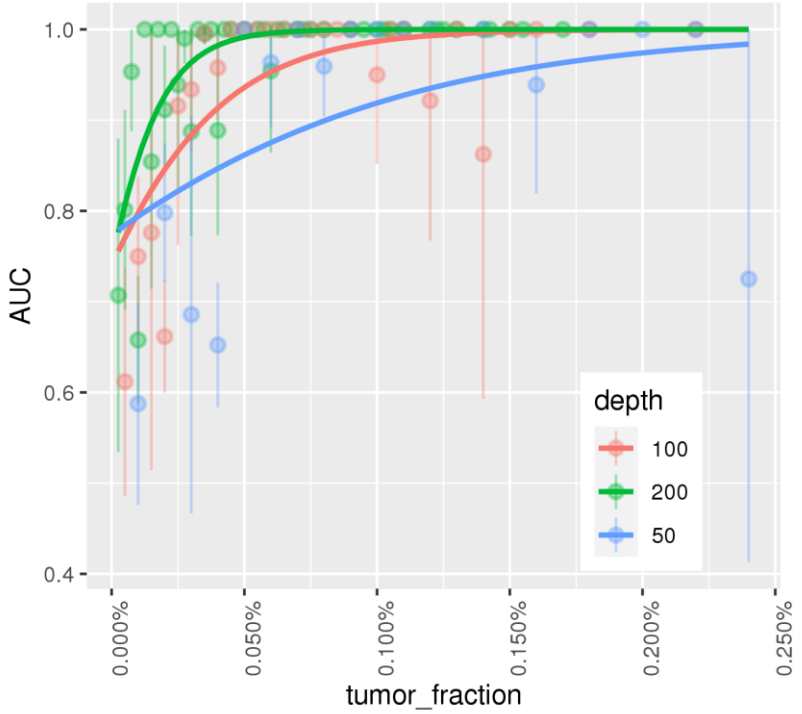

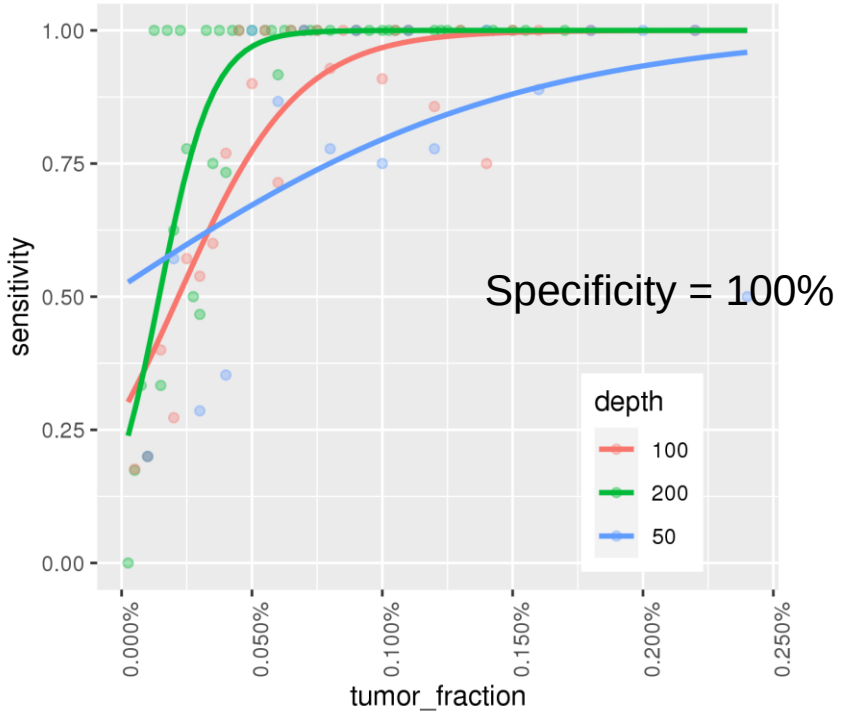

Simulation Results: second primary cancer detection

- No pre-surgery/treatment information used in this simulation
- 122 simulation cases with tumor fraction 0% to 7.7%
  - 50 remission + 72 second primary disease
- AUC > 80% when tumor fraction >= 1% at 200x

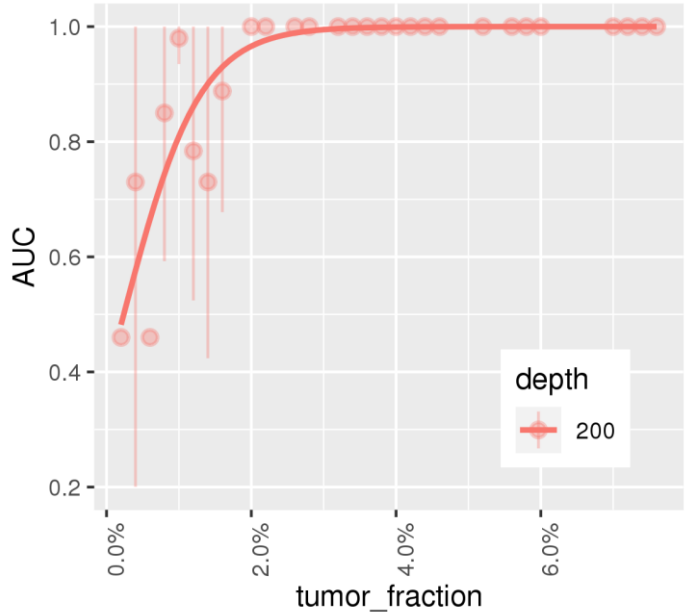

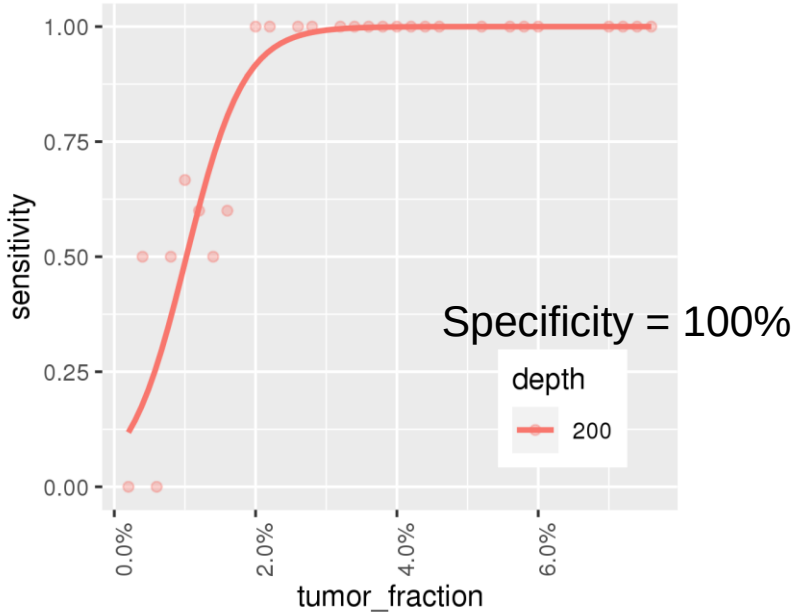

Develop a Methylome Test for the Early Lung Cancer Detection

Our "All-in-One" methylome-based diagnostics

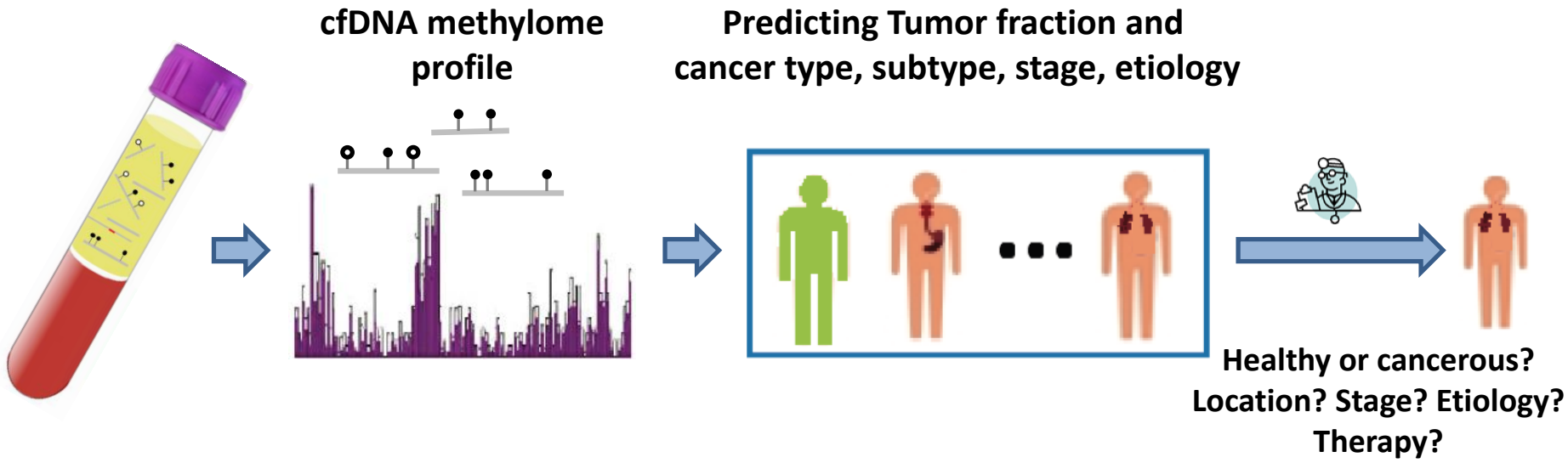

- ✓ **Robust and sensitive**
- ✓ **Low cost**
- ✓ **"All-in-One" blood test**
  - ✓ **Detecting cancer**
  - ✓ **identifying possible cancer location, stage, and etiology**
  - ✓ **predicting disease progression or therapy optimization.**

Our Exp+Comp Technologies

- ✓ **Experimental technology**: Novel sequencing library preparation method to reduce the cfDNA methylome sequencing cost by 15-20 folds

- ✓ **Computational technology**: Integrating multiple features and ensemble machine learning to identify trace-amount of tumor DNA signals in blood

Experimental Technology:
Reduce the methylome sequencing cost by 15-20 folds

We developed a *Reduced Representation Methylation Sequencing* technology, specifically tailored for cell-free DNAs. Specifically, we invented an innovative end-labeling technique, which bypasses the size selection step to enrich CpG islands, therefore achieving cost-effective methylome sequencing for cfDNA.

Integrative Prediction Model: Integrating multiple feature types for cancer detection

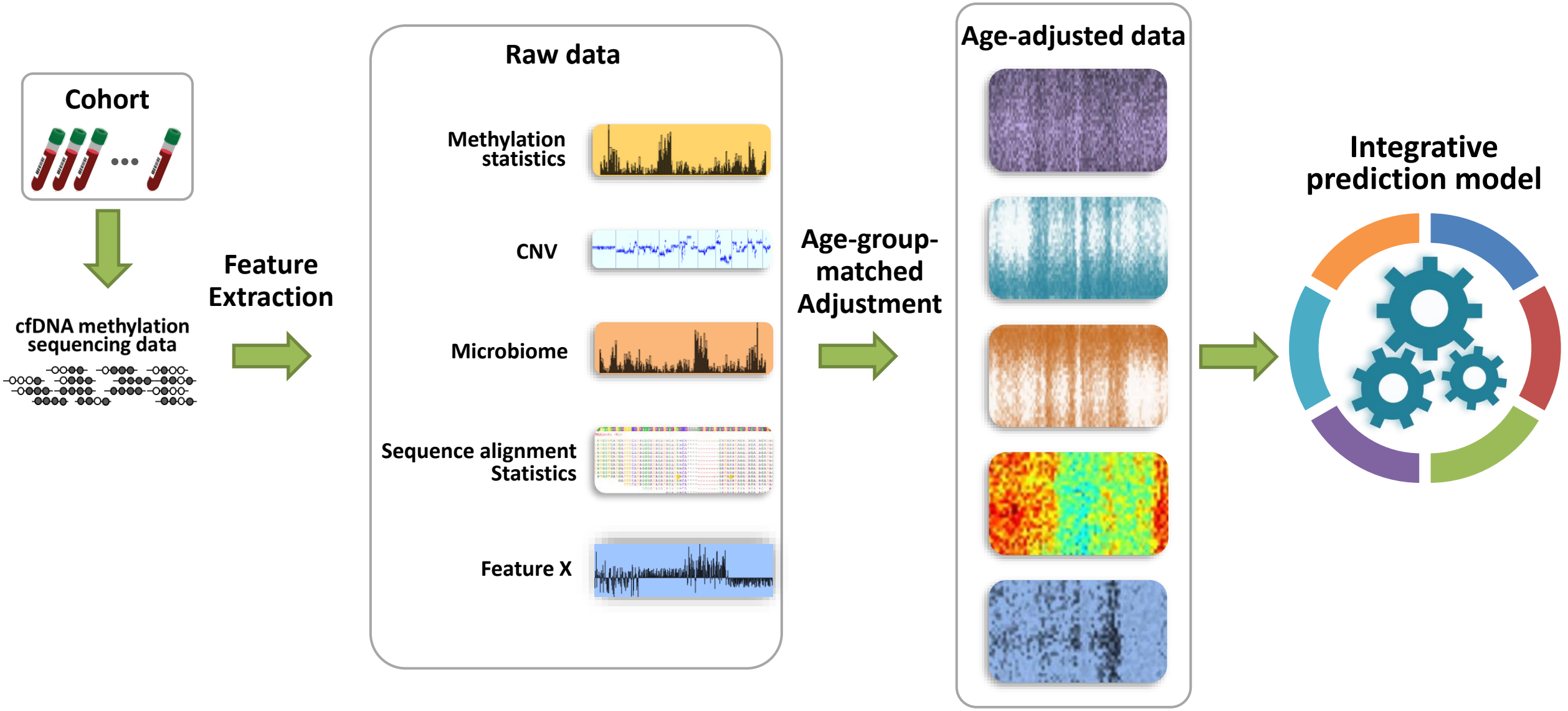

Sensitive detection of lung cancer

Age-adjustment (30): 30 non-cancer samples

- Six age groups: [20,30), [30,40), [40,50), [50,60), [60,70), [70,100]

Marker discovery (84): 38 non-cancer cfDNA samples & 46 lung tumor samples

Leave-One Out Cross-Validation (215): 117 non-cancer & 83 cases (26% Stage I, 18% Stage II, 23% Stage III, 33% Stage IV)

Results: at the Specificity of 99%,
90% sensitivity in detecting all-stage lung cancer,
89% in detecting early-stage cancer (Stage II,II, III)

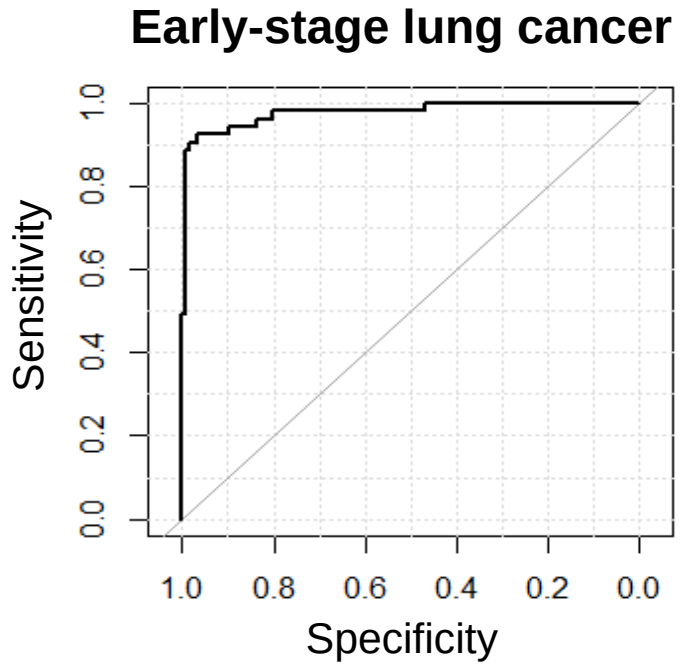

Potential for biomarkers of cancer risk from LUSC premalignant lesion associated gene expression

Extending the “field” to premalignancy (PML): Gene expression alterations associated with presence of lung squamous PML

RNA-seq on airway epithelium from 75 smokers with dysplastic lesions vs. 25 without apparent dysplasia (Stephen Lam UBC)

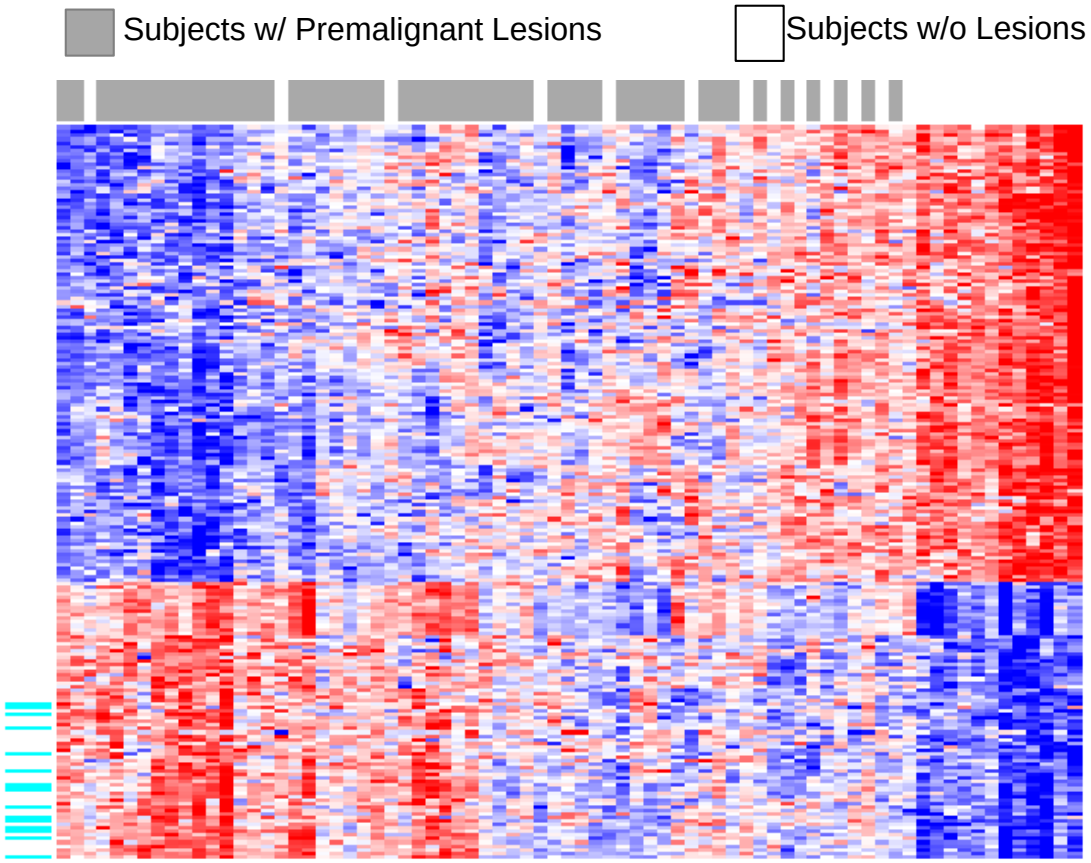

206 genes differentially expressed at FDR<0.001

Beane et al. Clinical Cancer Res 2017

Linking the "field" to the premalignant lesion via the Lung Pre-Cancer Atlas

(SU2C Dream Team; NCI PCA; JNJ)

Study Design

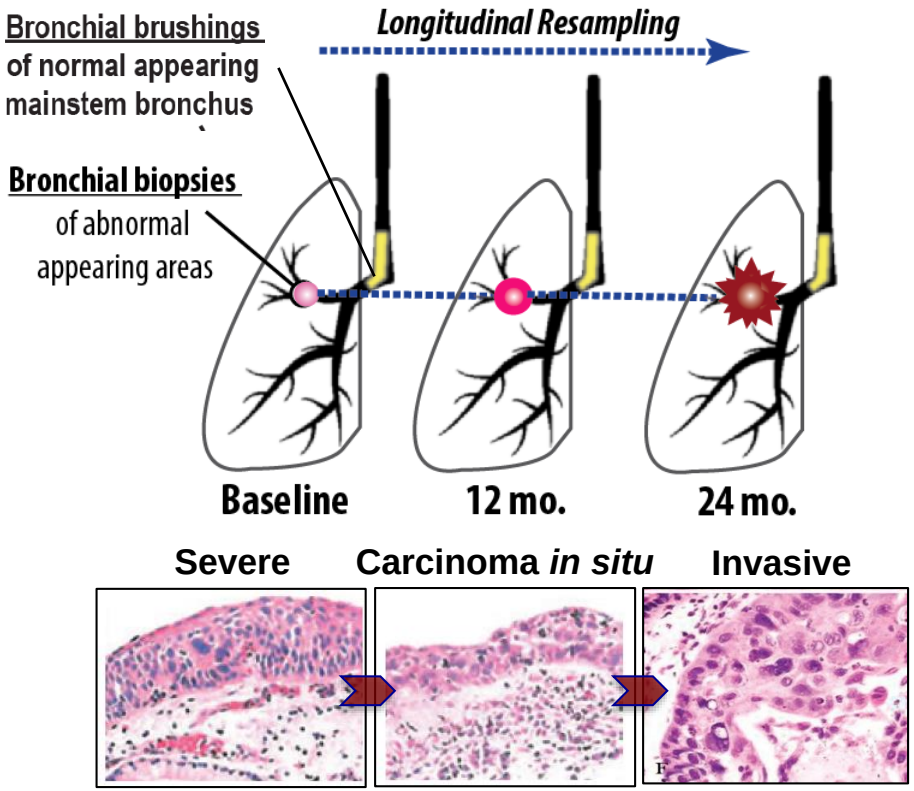

Biopsy-derived Molecular Subtypes

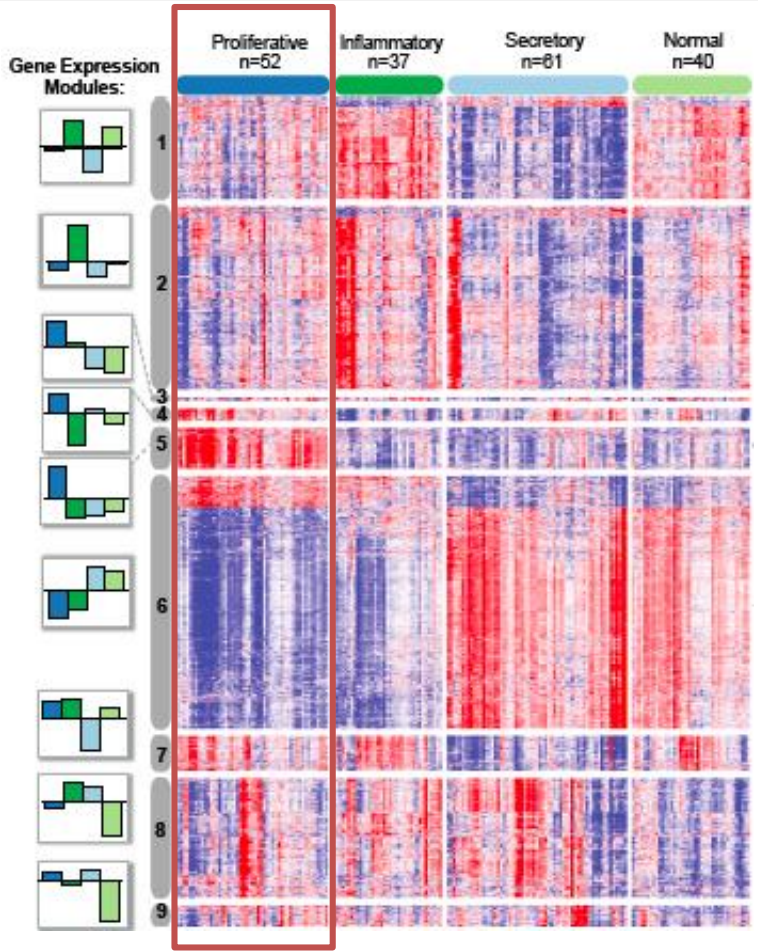

Bronchial Brushes Reflect Lesion Proliferative Subtype

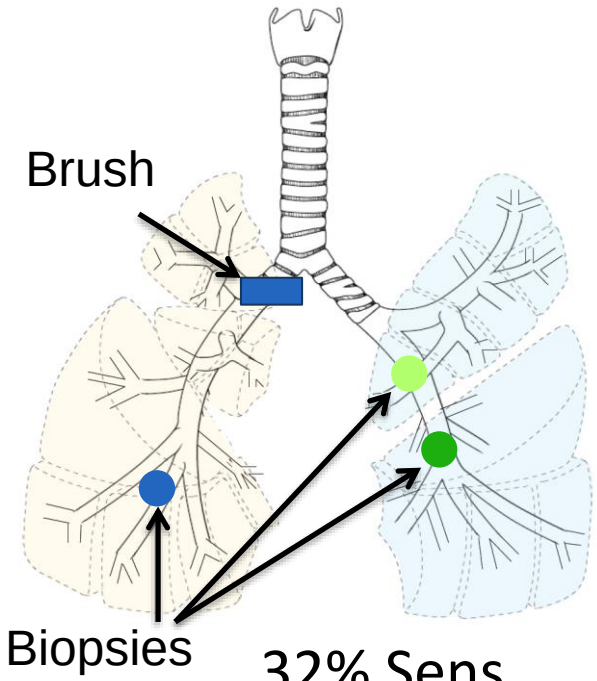

32% Sens.
91% Spec.

Beane et al. Nature Communications. 2019.

Immune-associated gene-expression module linked to progression in high-grade sqPML subtype

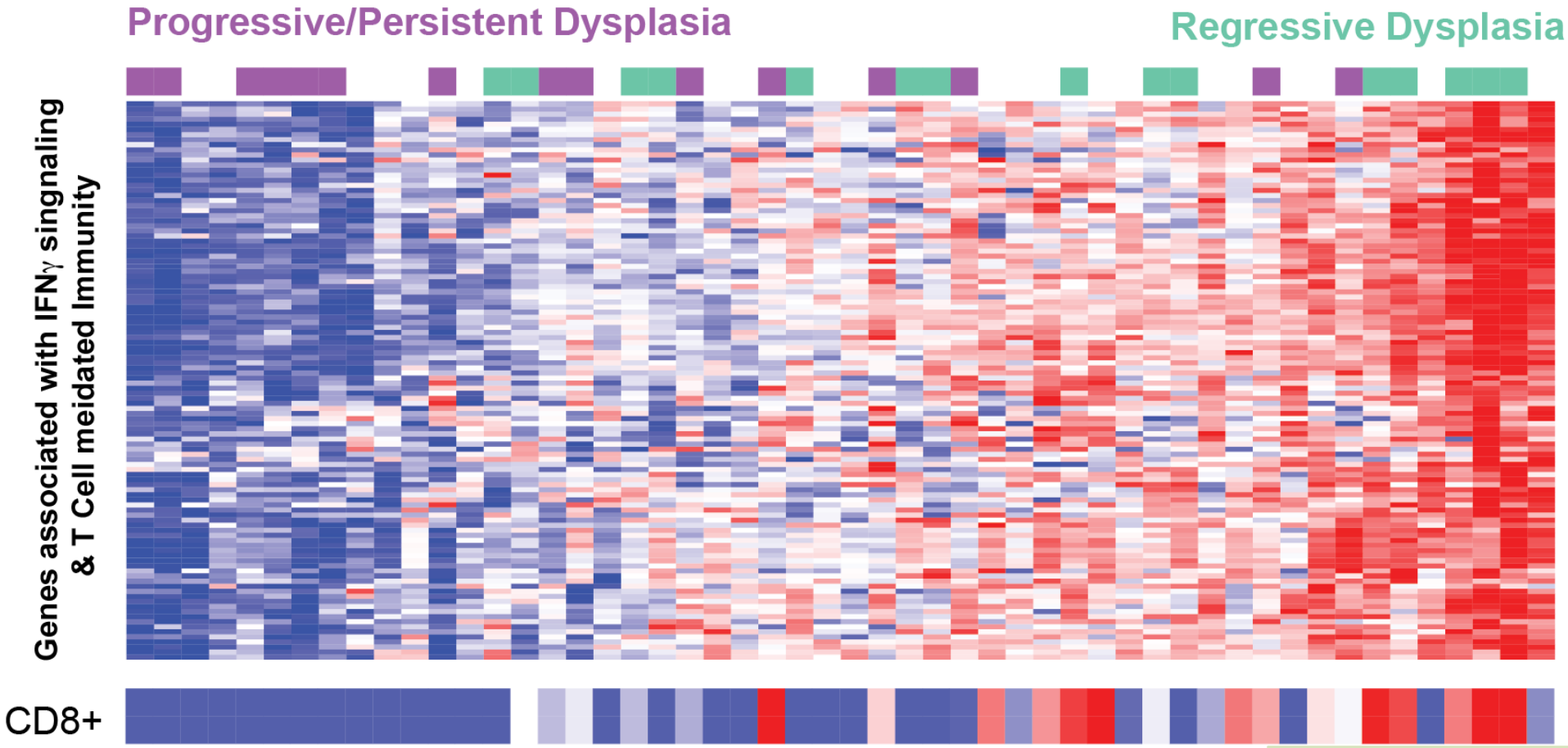

Potential to serve as a biomarker to predict indolent vs. aggressive lesions

Beane et al. Nature Communications. 2019.

Premalignancy biomarkers for assessing cancer risk

- Biomarker for detecting PML
- Biomarker for detecting high-grade PML subtype
- Biomarker for detecting progressive high-grade PML

- Molecular characterization of PML also provides insights into carcinogenesis and therapeutic targets

How can understanding the immunopathogenesis of lung cancer lead us to early detection and interception?

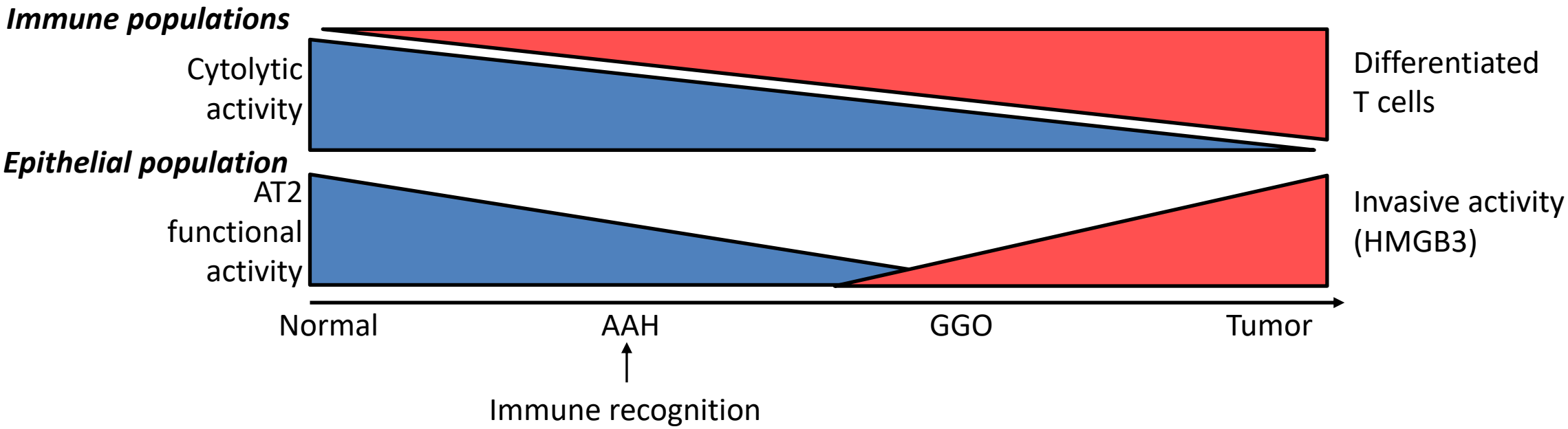

The immune response shapes the developing tumor

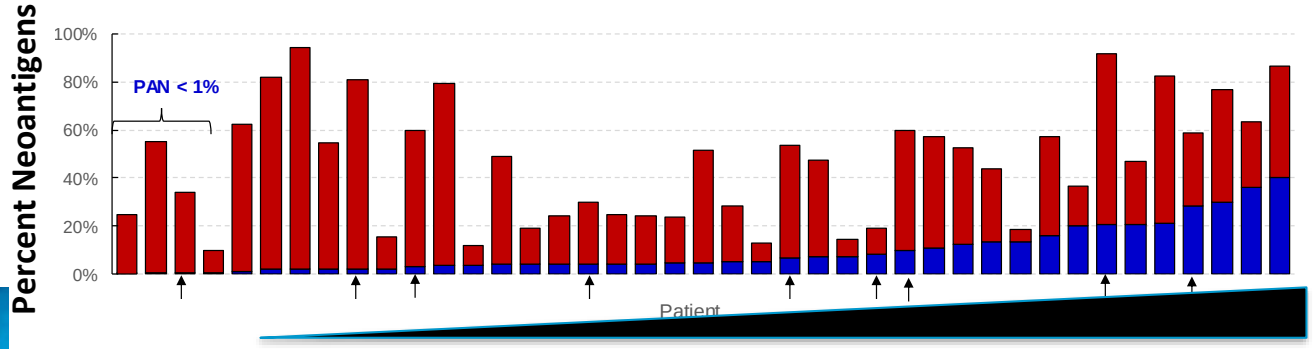

Malignant Specific Neoantigens (MSNs)

Progression Associated Neoantigens (PANs)

CD8 + T-cells in AAH Region

Kostyantyn Krysan

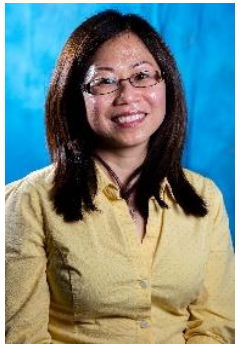

Linh Tran

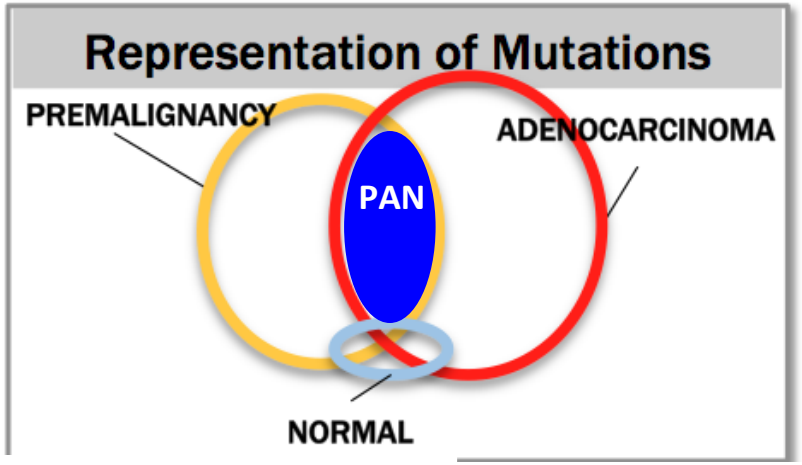

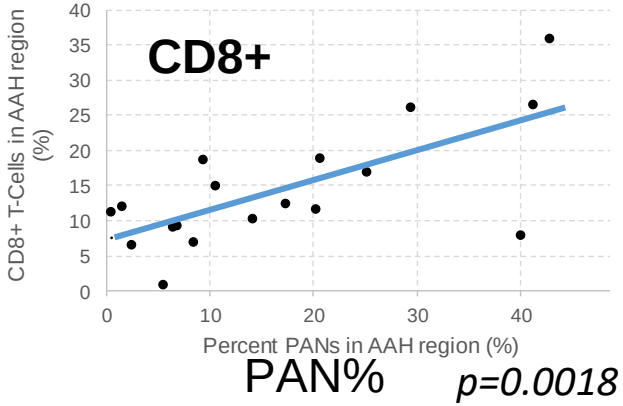

PAN% *p=0.0018*

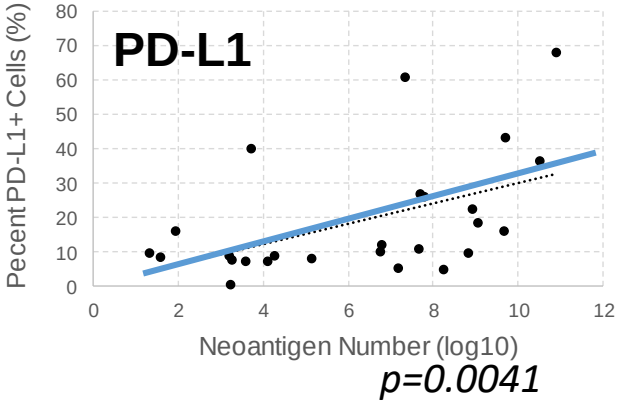

p=0.0041

DAPI PD-1 PD-L1 CD8

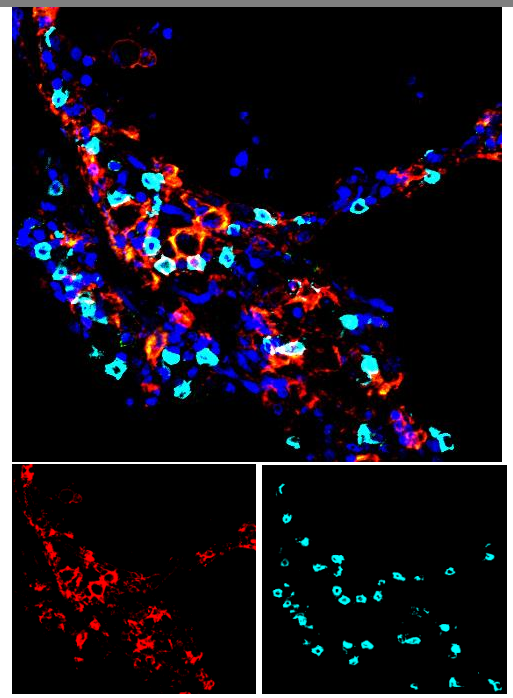

Krysan et al. Cancer Research 2019

Single cell transcriptome profiling of ground glass opacities (GGOs)

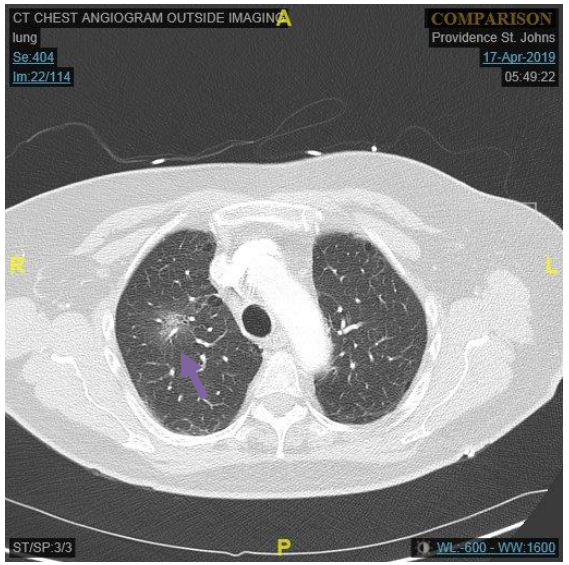

Patient #3. GGO

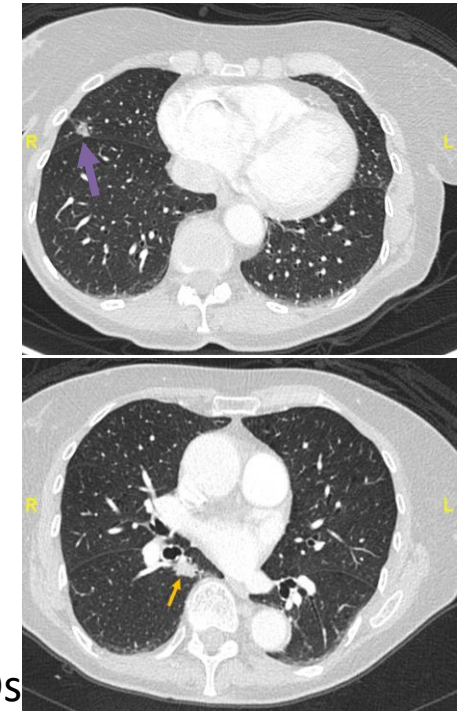

Patient #4. 2 GGOs

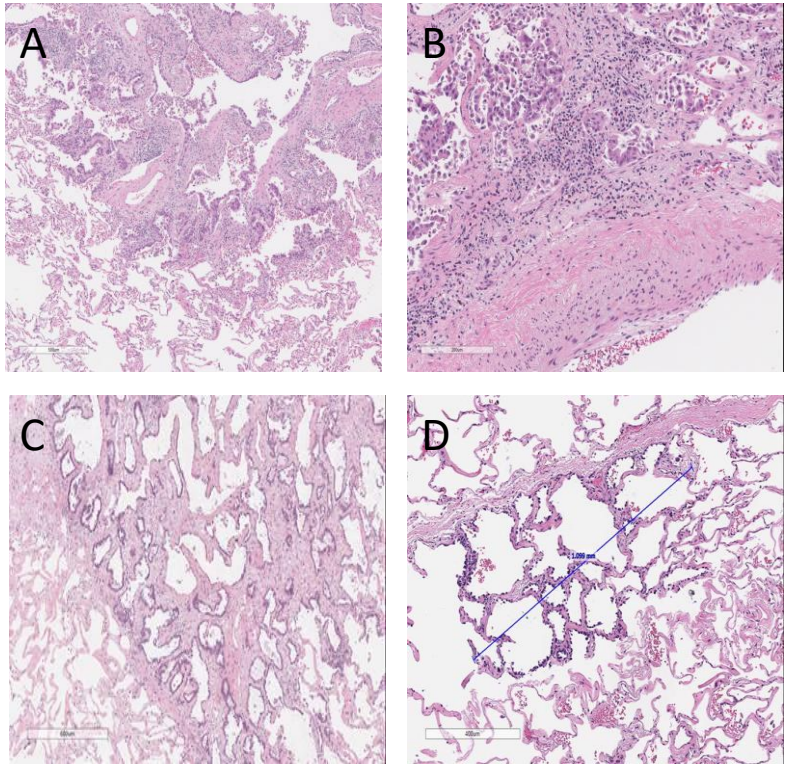

- Total of 6 cases (15 samples) were processed for scRNA – Seq
  - Two cases with multiple lesions (e.g. case 4 with 2 GGOs and one solid tumor)
  - Normal and abnormal lesions were collected
- Immune profiles were heterogenous among subjects
  - High immune infiltration in GGO in case #1 (**A** and **B**)
  - Very low immune infiltration in GGO (**C**) and AAH (**D**) in case #2.

Clinical features of six GGO patients

Pt	Lesion type by CT	Gender	Smoking status	Age	Ethnicity	Post-surgery diagnosis	Size/invasive component, mm	Driver mutations	Stage
1	GGO	F	Never	72	Caucasian	ADC	12	EGFR E19 del	T1bN0
2	Solid	F	Former	74	Caucasian	ADC, AAH	15	KRAS G12D	T1bN0
	GGO					MIA	11/3	KRAS G12F	
3	GGO	F	Former	77	Caucasian	ADC	31/25	KRAS G12V	T1cN0
4	Solid	F	Former	76	Caucasian	ADC	16	EGFR E20 ins	T1bN1
	GGO#1					ADC	13/9		
	GGO#2					ADC	6	KRAS G12V	
5	GGO	F	Former	68	Caucasian	MIA, AIS, AAH	18	EGFR L858R	T1miN0
6	GGO, semi-solid	M	Former	76	Asian Indian	ADC	15	EGFR L858R and K860I	T1bN0

Immune cell profiles in early stage ADC

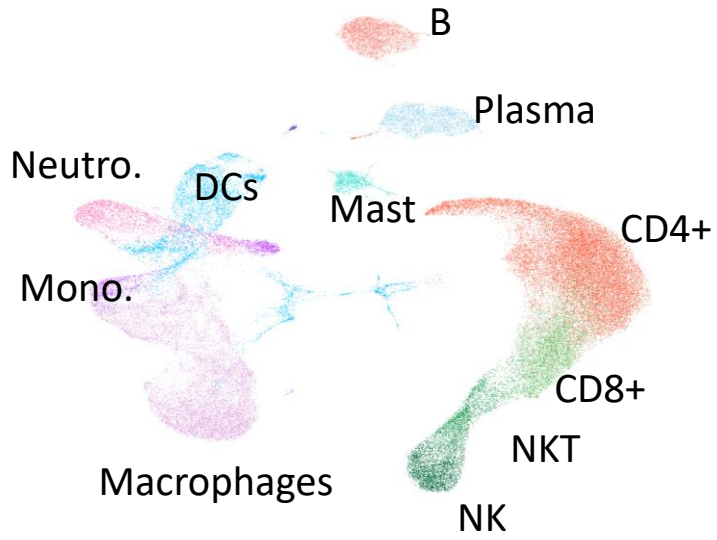

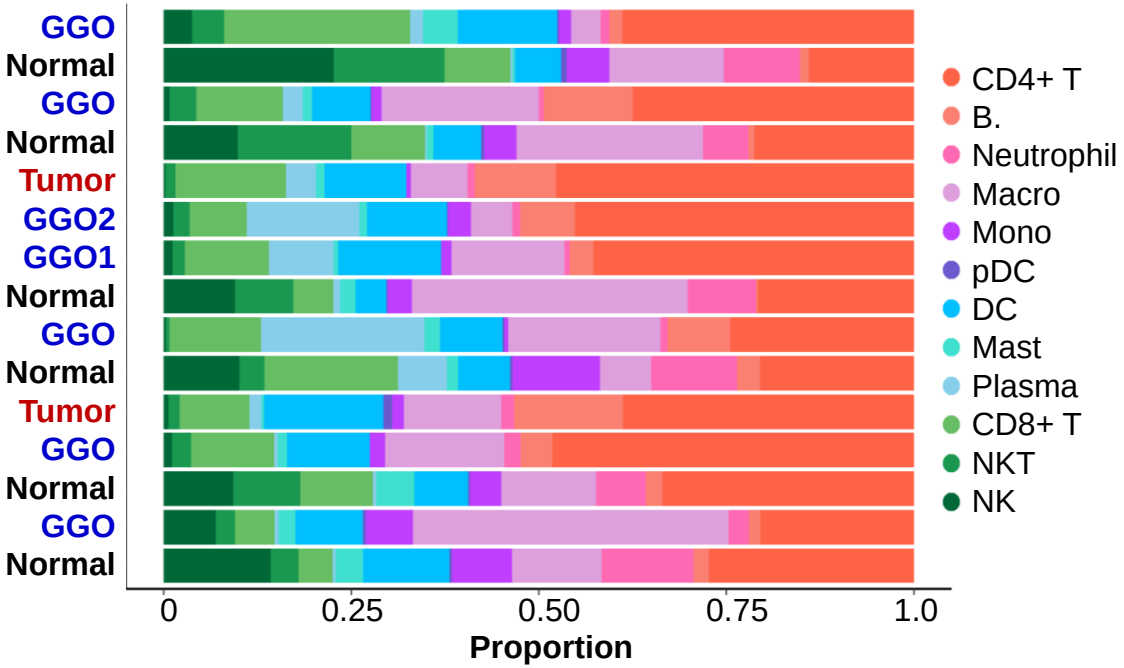

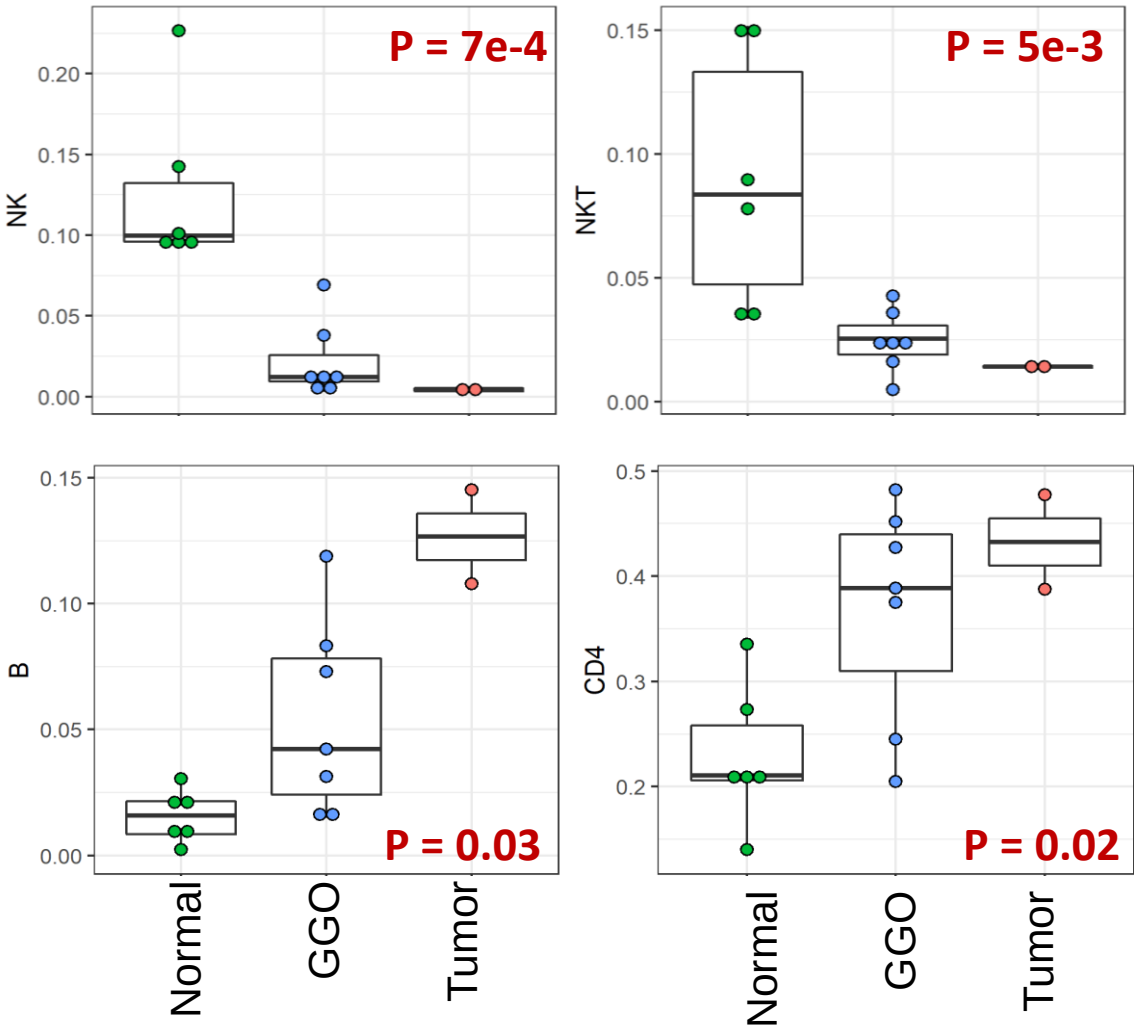

Decrease in innate immune responses (NK/NKT cells) and increase in adaptive responses (CD4+ T and B cells) in early stage ADC

Reduction in NK and NKT cytolytic capacity in early stage ADC

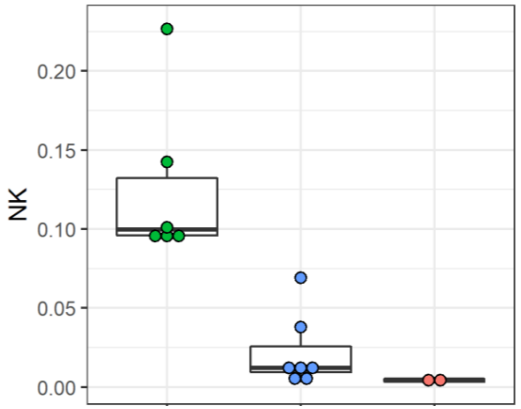

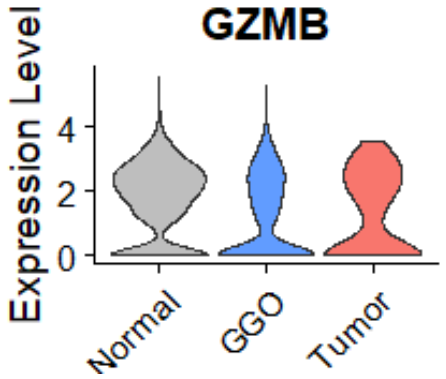

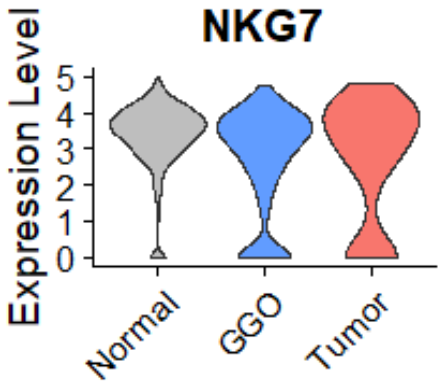

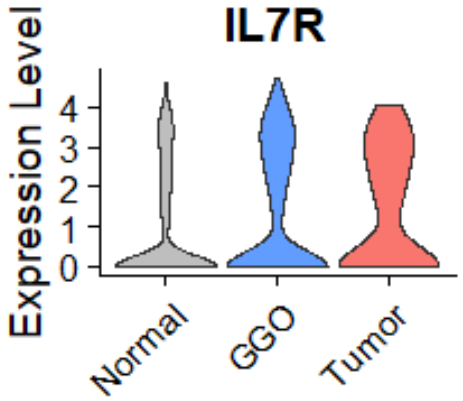

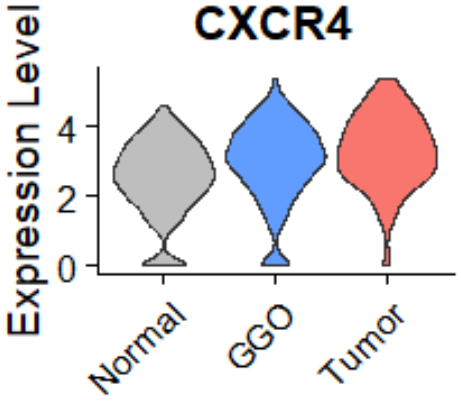

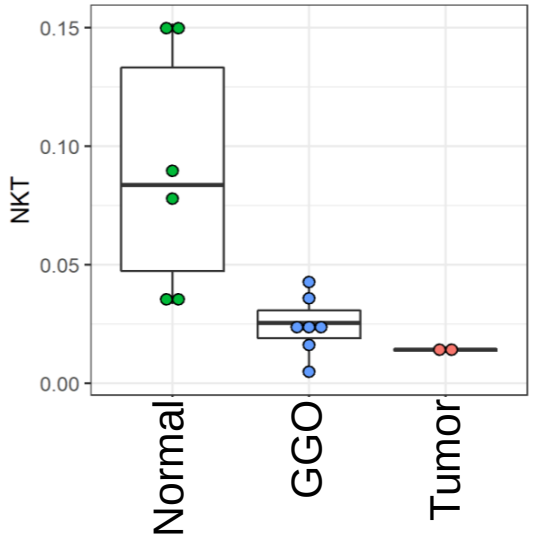

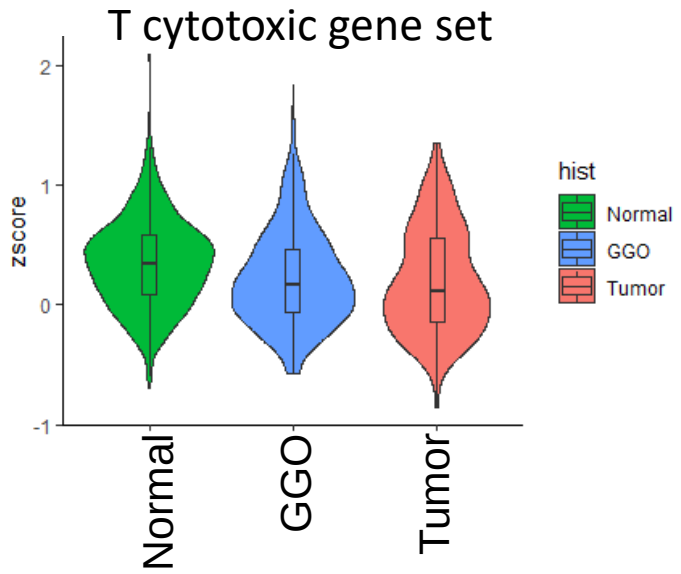

NK and NKT cells show decreased expression of GZMs and express differentiation markers (IL7R and CXCR4 receptors) in GGOs and tumors

Increase in CD4+ T-reg in early stage ADC

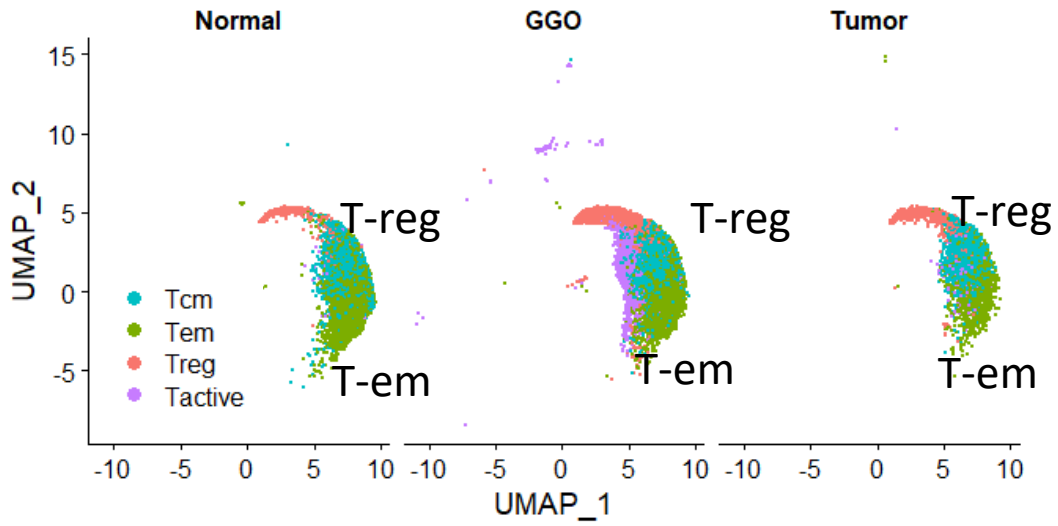

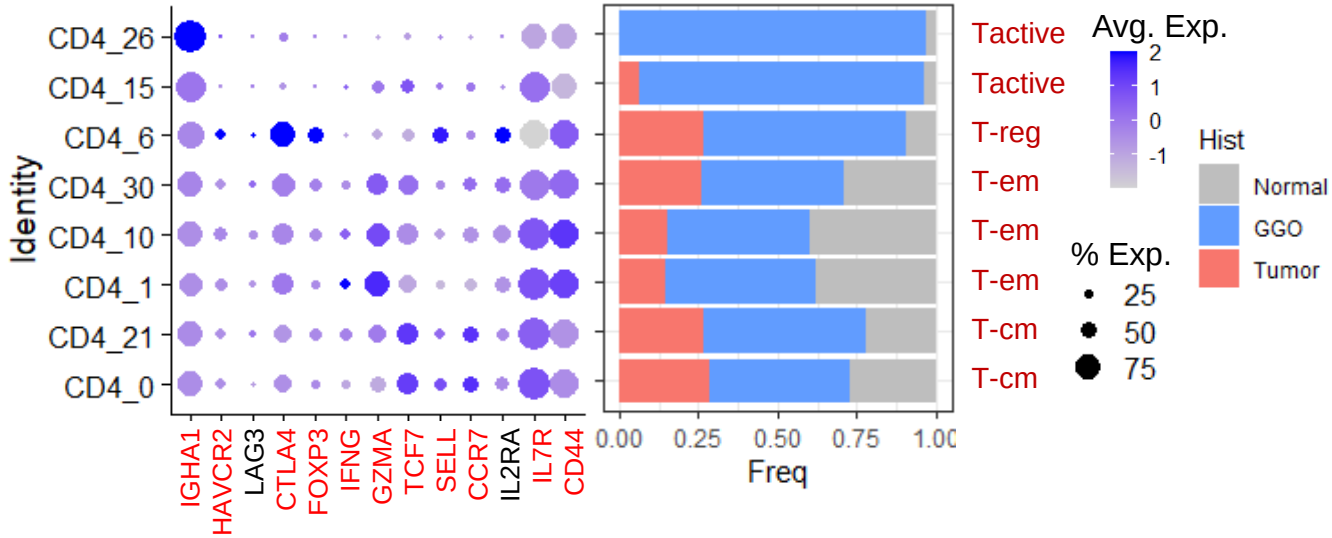

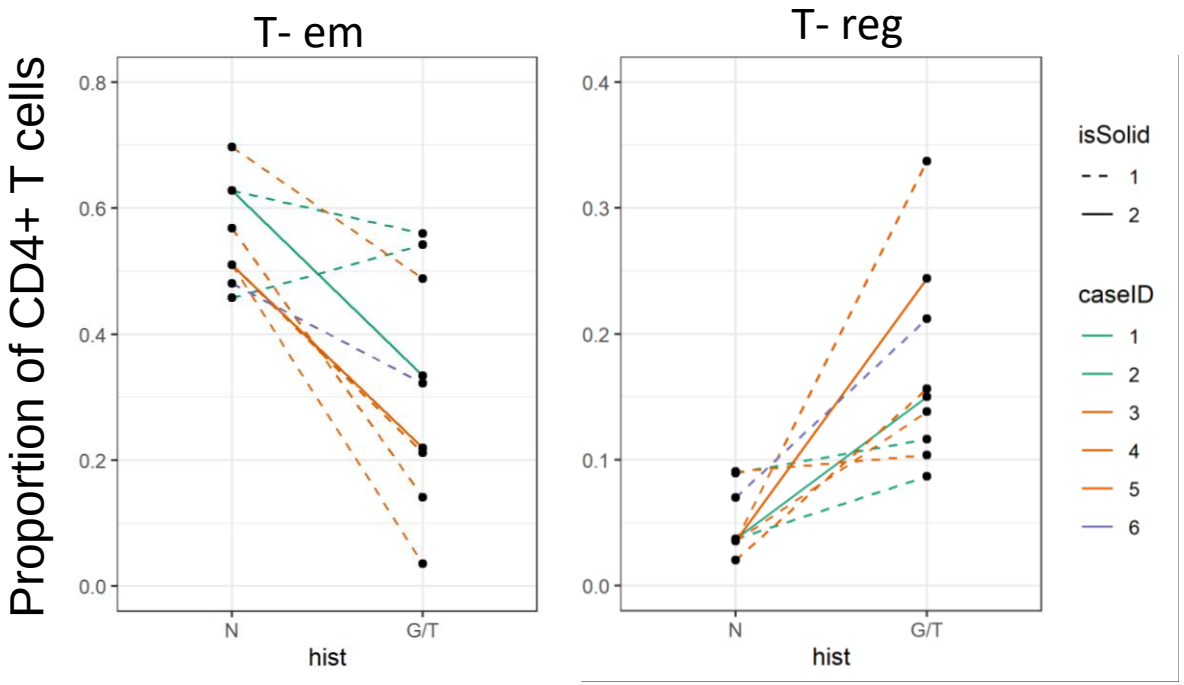

- CD4+ T cell population did not only increase, but also changed their composition in GGOs and tumors
- T-reg component increased significantly, and T effector memory component decreased in GGOs and tumors compared to normal
- In two cases having tumors in addition to GGOs, the magnitude of change in tumors was higher than GGOs

Non-Immune cell profiles in early stage ADC

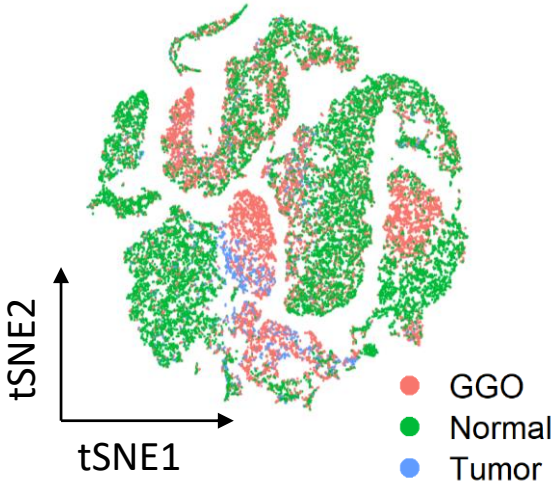

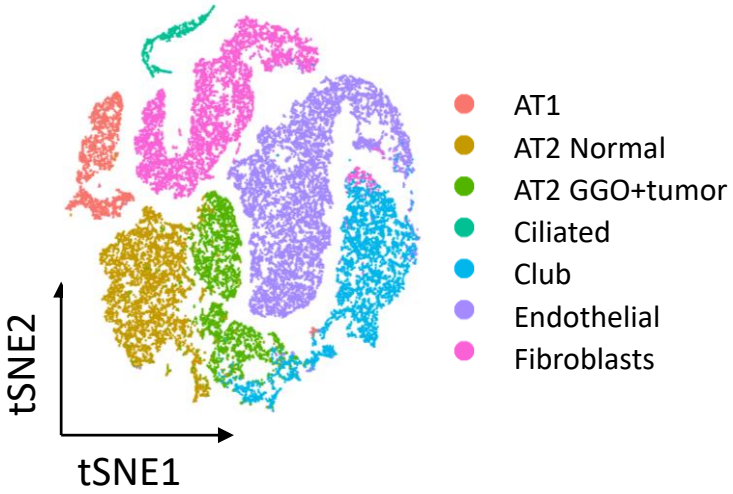

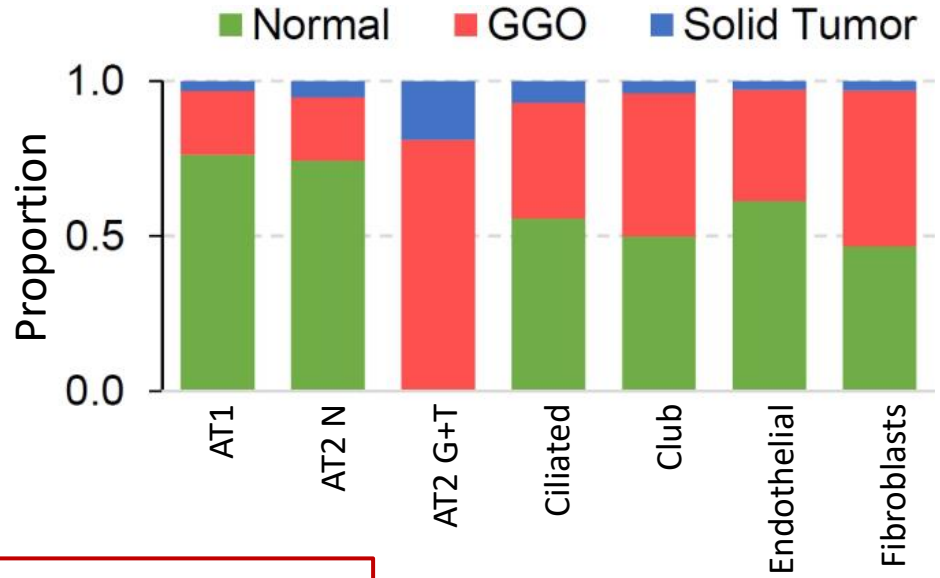

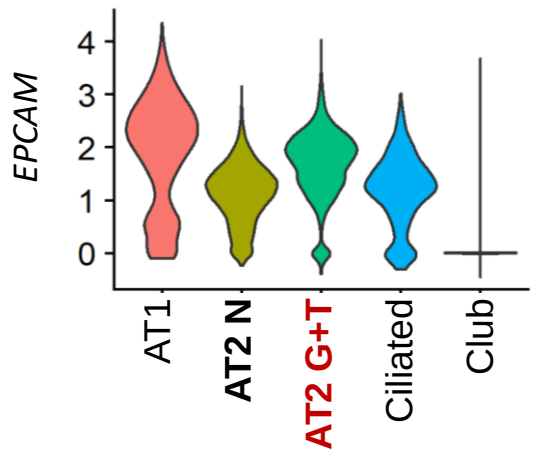

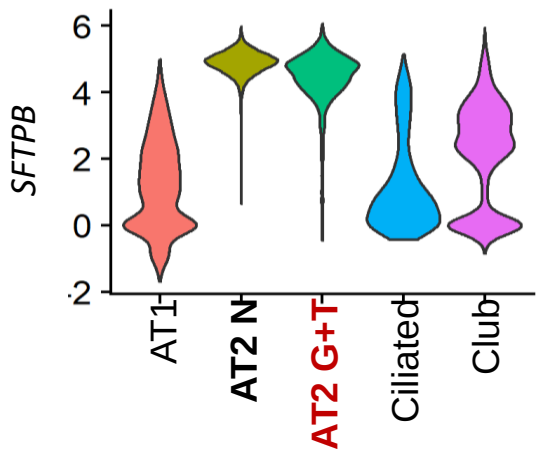

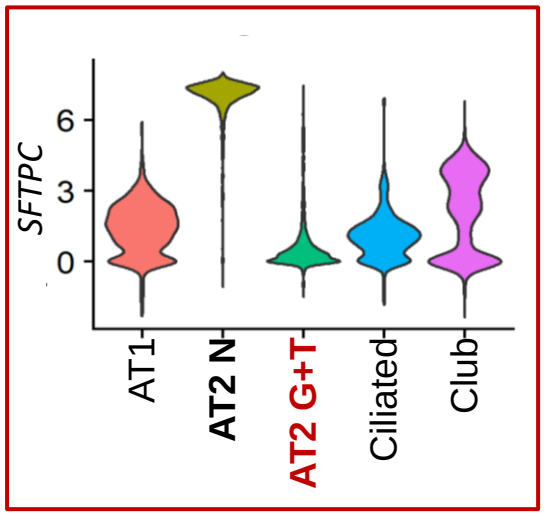

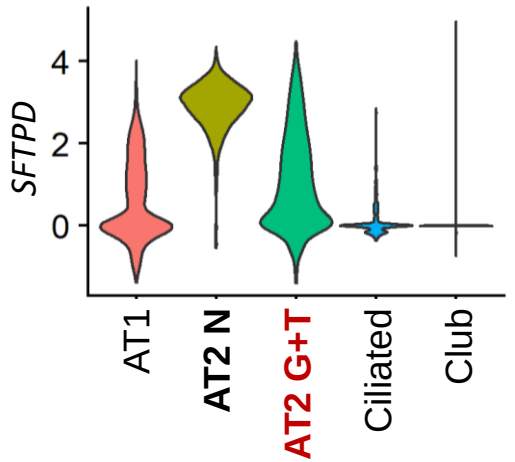

AT2 cells reduced the expression of their critical functional protein surfactant in the early stage of ADC

DEGs in AT2 cells in early stage ADC

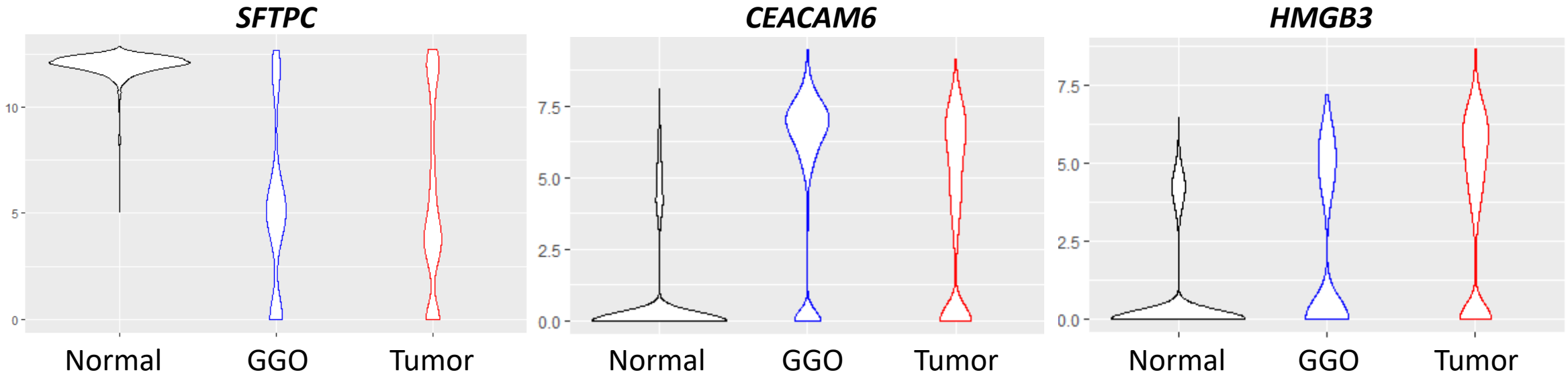

143 up-regulated genes involved in

- Extracellular matrix proteins
- p53 pathway proteins

Summary

Immune cell profiling of the early stage ADC demonstrated:

- Significant reduction in NK and NKT cells suggested changes in the innate immune response
- Increase of CD4+ T cells and B cells with up-regulation of T-reg
- Immune surveillance was reduced and immune editing was increased in early stage ADC

Non-immune cell profiling of the early stage ADC demonstrated:

- Reduction in the expression of AT2 cell differentiation maker genes (*SFTPC*, *SFTPD*) indicated altered functions of AT2 cells from tumors
- Deregulation of extracellular matrix genes suggested changes toward increased invasiveness

EDRN's future impact on the global burden of lung cancer mortality

- **2.2 million incident cases of lung cancer per year**
- **1.9 million deaths per year**
- **Between 2007 and 2017 lung cancer cases increased by 37% worldwide.**

A Systematic Analysis for the Global Burden of Disease Study
JAMA Oncology 2019

Disparities:

Racial/ethnic disparities in lung cancer screening
Tailor et al Chest 2020, Lake et al BMC 2020

Acknowledgments

Boston University
Marc Lenburg
Avi Spira
Jennifer Beane
Joshua Campbell
Sarah Mazzilli
Grant Duclos
Jiarui Zhang
Boting Ning
Xingyi Shi
Xu Ke
Eric Burks
Elizabeth Moses

Vanderbilt University
Pierre Massion

University of California Los Angeles
Steve Dubinett
David Elashoff
Jasmine Zhou
Michael Fishbein
Kostyantyn Krysan
Linh Tran
Bin Liu
Denise Aberle
William Hsu
Matthew Brown
Ashley Prosper
Greg Fishbein
Raymond Lim
Manash Paul
Camelia Dumitras
Zhe Jing
Christopher Sundberg
Ramin Salehi-Rad
Rui Li

Roswell Park Cancer Institute
Mary Reid
Sai Yendamuri
Mark Hennon

Lahey Clinic
Carla Lamb
Kimberly Reiger-Christ
Travis Sullivan

MD Anderson Cancer Center
Ignacio Wistuba
Humam Kadara
Junya Fujimoto
Beatriz Sanchez Espiridion

J&J
Chris Stevenson
Duncan Whitney
Jessica Vick